DISCUSSION PRÉPARÉE / VORBEREITETE DISKUSSION / PREPARED DISCUSSION

Specifications on Multi-Story Buildings and in Particular on Steel Structures in Seismic

Recommandations pour le calcul des bâtiments à plusieurs étages en zone sismique avec référence spéciale aux constructions en acier

Empfehlungen für mehrstöckige Gebäude, insbesondere für Stahltragwerke in Erdbebengebieten

ELIO GIANGRECO
Italy

The Convention of European Constructional Steelwork Associations has appointed a special Commission for compiling the "Recommenda - tions" for the design of steel structures in seismic area.Such Commission, known as Commission XIII, has begun his works in 1965 and in a first stage has accurately studied all international standards on the argument by making comparison and analysing those parts that the different recommendations have in cpmmon.

On the basic of the aquired knowledges and taking into account the most recent standards, the Commission has outlined a text of recommendations with comments where the general principles of the standards have been explained and some particular cases have been treated. Numerical coefficients have also been given. The Commission has decided that buildings in seismic area can be designed only if the equivalent static forces proportional to the masses in motion through a suitable seismic coefficient are introduced.Such coefficient has been fixed on the basis of the most recent studies of seismic engineering based on the spectral analysis of earthquakes and has been considered as the product of four elementary factors: the intensity seismic factor, the foundation factor, the response factor and the masses distribution factor.

The influence of each factor has been pointed out both from a qualitative and a quantitative point of view by introducing suitable schemes and simplified formulations.

In the text have also been treated the problems of torsional actions due to seismic motions as well as the stresses due to vertical actions.

Studies for preparing a further chapter on the efficiency of connections between members both of the up structure and of the foundation structure are going on. In examining the factors which define the seismic factor the Commission has paid a particular at

tention to the evaluation of the response coefficient of the structures. As it is known this coefficient depends on the natural period of vibration of the structure as it is shown by the spectral analysis of the earthquakes.

In the following it has been reported on some researches carried out for the evaluation of the natural period of vibration of buildings.

- Period of vibration of framed structures

Because of the difficulties of evaluating the natural period of vibration, simplified formulations have been suggested by some Authors which relate the period T to the number of floors of a building, and sometimes to its geometric and elastic characteristics.

Among the most widely used formulae, the following ones may be listed:

$$T = 0,1\ n,$$

and:

$$T = \frac{0,05}{\sqrt{D}}\ H$$

which are respectively used by S.E.A.O.C. standards for framed structures and structures with stiffening walls.

In the formulae above, n represents the number of floors, and H and D respectively the height and the transversal dimension of the building in feet.

It is worth writing also the formula suggested by Ifrim for plane frames:

$$T = \frac{2\pi}{\xi}\sqrt{\frac{M_o\ l_o^3}{E\ J_o}} \qquad (1)$$

where M_o, l_o and J_o are spectively the base mass lenght and moment of inertia, E the elastic modulus of the material and ξ a parameter which depends on the number of floors and columns as well as on the masses and stiffnesses distribution on the height.

In order to check the validity of the proposed formulations some studies on the argument have been carried out in the "Istituto di Tecnica delle Costruzioni" of the University of Naples.

Firstly plane structures with or without windbracing have been considered; secondly a dynamic analysis of three dimensional frames has been undertaken.

1) - Plane structures

For plane structures a sistematic theoretic study has been carried out by releasing all simplifying hypothesis formulated in the papers dealing with the argument. In fact either the possibility of joints to rotate and the inertial forces acting on each beam have been taken into account. The latter circumstance requires an iterative process if the elastic characteristics vary with the period of vibration.

If a value of the lowest frequency is fixed (in particular it has been assumed the value corresponding to infinitely rigid beams and weightless columns hypothesis) it is possible to calculate the functions rectifying the elastic characteristics of all rods. Next

a unit displacement is given to all the joints of the structure, one per time, and the structure is solved each time. Then the matrix of the reactions of fictitious supports is obtained.

As it is known the n eigenvalues are proportional to the n squares of natural vibration of the structure. Comparing the lowest of the eigen values with the one fixed, a new iteration process can be carried out assuming the new frequency as starting value.

The investigation has been extended to frames with a number of floors ranging from 2 and 24, and with a number of spans m between 1 and 14.

In a first stage frames with fixed joints and without windbracing have been considered; then the analysis for braced structures has been formulated. With regard to common frames the fundamental period of vibration depends obviously on the number of floors and spans as well as on the variation law of moments of inertia on the height of the frame, on the inertia of beams and on the mass of all rods. The analysis of design characteristics of several steel buildings has suggested some variation laws of the cross section of columns with the height and consequently of their masses. With regard to beams the variation of their moment of inertia with the height does not seem to seriously influence the value of the period of vibration.

Using the Computer it has been possible to calculate the frequencies of vibration of a large number of frames whose geometric characteristics range as stated before. Besides it has been tried to find a variation law of the unknown parameter as function of the data.

With regard to unbraced frames the following expression has been obtained for the period of vibration:

$$T = 2\pi l_o^2 \sqrt{\frac{\mu_o}{E\ J_n}}\ T' \qquad (2)$$

where l_0 is average height of columns, J_n the moment of inertia of the columns of the last floor, μ_o the distributed mass of the beam.

The quantity T' given by graphs on fig. 1 and 2 for 1 and 14 spanned frames respectively, can be expressed by:

$$T' = 0{,}31 + f(\alpha)\ n - \frac{1{,}3\ m^3}{10^m}$$

where n is the number of floors, m the number of spans and $f(\alpha)$ is related to the variation law of moments of inertia of columns with the height of the frame through the expression:

$$\frac{J_i}{J_n} = \alpha\ (n-i) + 1 \qquad (3)$$

Obviously if the behaviour of the J_i/J_n is not linear a suitable value for α has to be chosen which is able to better approximate the exact curve. Function $f(\alpha)$ is shown in fig.3.

With regard to the variation laws of moments of inertia 3 and 4 in fig. 1 and 2 some comparison have been made with the formula sug

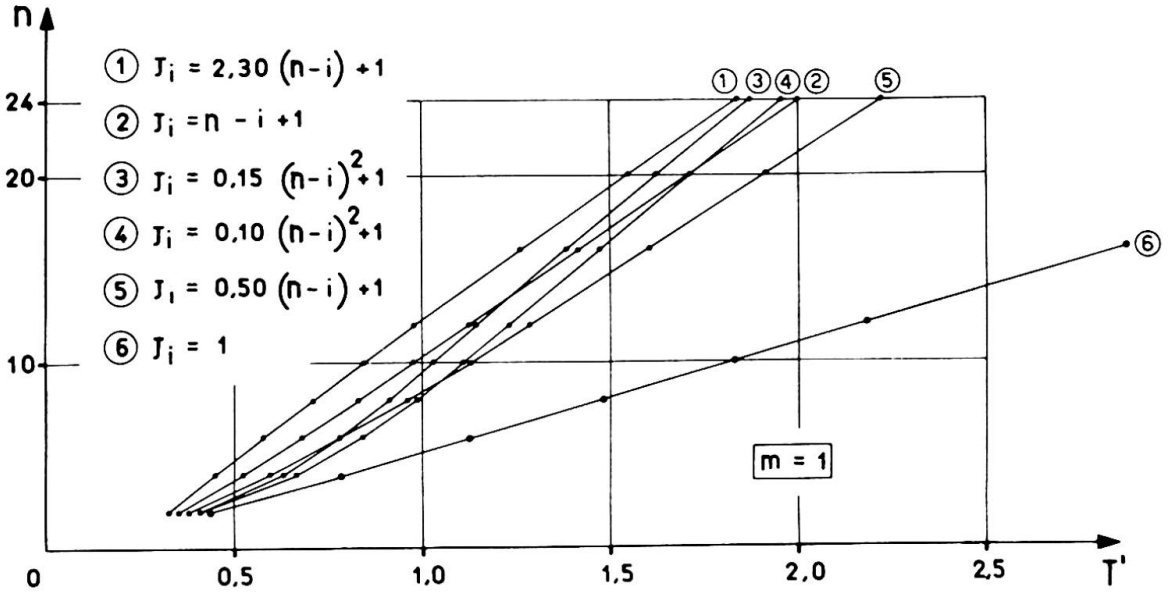
n
24
20
10
0
0,5
1,0
1,5
2,0
2,5
T'
① $T_i = 2,30\,(n-i) + 1$
② $T_i = n - i + 1$
③ $T_i = 0,15\,(n-i)^2 + 1$
④ $T_i = 0,10\,(n-i)^2 + 1$
⑤ $T_i = 0,50\,(n-i) + 1$
⑥ $T_i = 1$
m = 1

Fig. 1

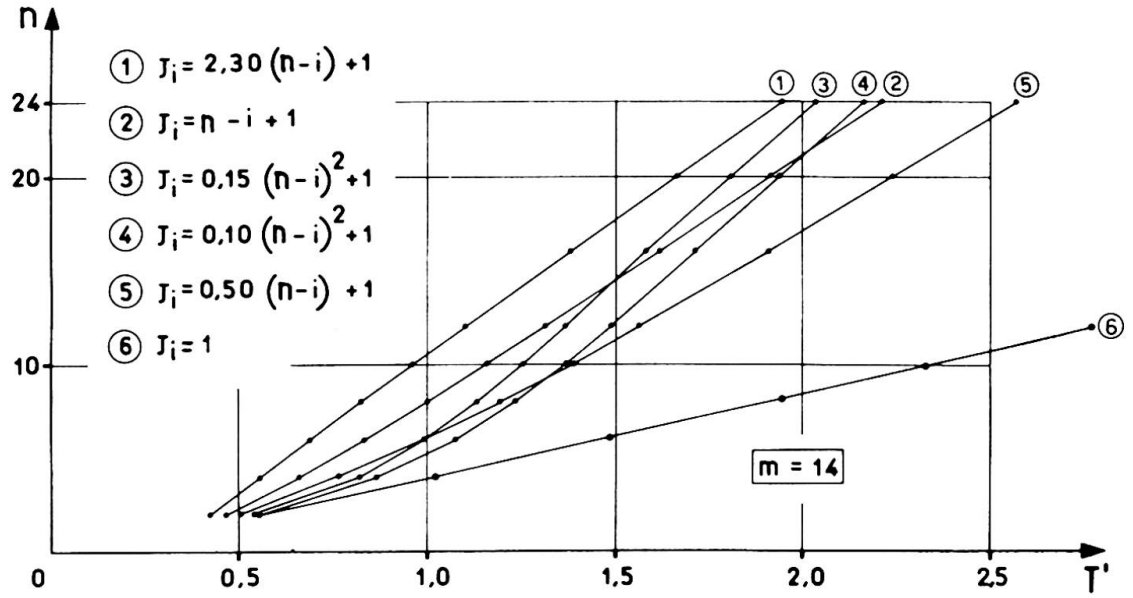
n
24
20
10
0
0,5
1,0
1,5
2,0
2,5
T'
① $T_i = 2,30\,(n-i) + 1$
② $T_i = n - i + 1$
③ $T_i = 0,15\,(n-i)^2 + 1$
④ $T_i = 0,10\,(n-i)^2 + 1$
⑤ $T_i = 0,50\,(n-i) + 1$
⑥ $T_i = 1$
m = 14

Fig. 2

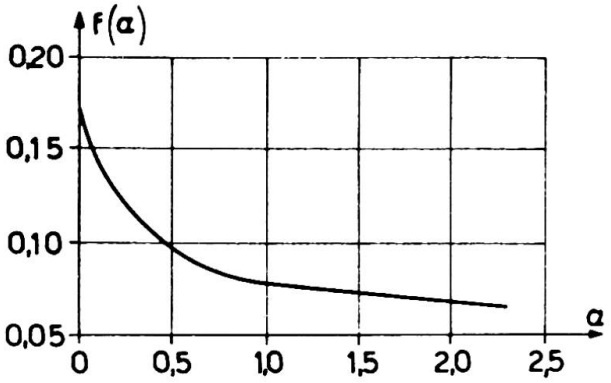

Fig. 3

gested by Housner and Brady:

$$T = 1{,}08\sqrt{n} - 0{,}86$$

and with that one by Ifrim (1) previously mentioned (fig.4 and 5).

In the same graphs concerning 1 and 14 spanned frames, both tha values obtained through calculations and those derived by using (2) are shown. Finally a qualitative graph shows what one might obtain if beams were infinitely rigid.

Later the investigation has been extended to braced frames with beams arranged according to "St. Andrew's Cross". It is assumed that beams are weightless and so slender that cannot absorb any thrust.

The procedure which has been followed is practically the same of that for ordinary frames. The difference consists in the fact that the matrix of stiffnesses of which are sought the eigenvalues is obtained as summation of two distinct matrices: the first one concerning the rods of structures and derived as before; the second one regarding the rods of bracing. The latter is tridiagonal because is independent on the rotation of joints and is invariant during calculations iterations. Such matrix can be immediately calculated and depends on the cross section area of rods as well as on the geometric dimensions of the mesh.

Introducing the equivalent moment of inertia:

$$J_e = \frac{A\, l^2 \sin^3 \phi}{12}$$

where:

A is the area of cross section of bracing rod;
l the width of the mesh;
ϕ the slope of bracing rods with respect to the horizontal, one has that the second stiffnesses matrix looks formally the same than that relative to frames with infinitely rigid beams.

Also in this stage several numerical examples have been carried out. Investigations have been performed on 1 to 14 spanned frames and with number of floors ranging from 2 to 24. Besides different variation laws of the moment of inertia on the height of the building and different stiffness ratios have been considered.

From the analysis of the results it seems still possible to apply the (2) if J_n is replaced by the fictitious moment of inertia

$$\bar{J}_n = J_n + \frac{\Sigma J_{e,n}}{m+1}$$

$\Sigma J_{e,n}$ is relative to the equivalent moments of inertia of all bracing rods of the last floor.

Similarly the parameter α will be still defined through the (3) where J_i and J_n must be replaced by $\bar{J}_i$ and $\bar{J}_n$. In such a way the equivalent moment of inertia of bracing rods has been "distributed" to all the columns at each floor, making still valid the (2).

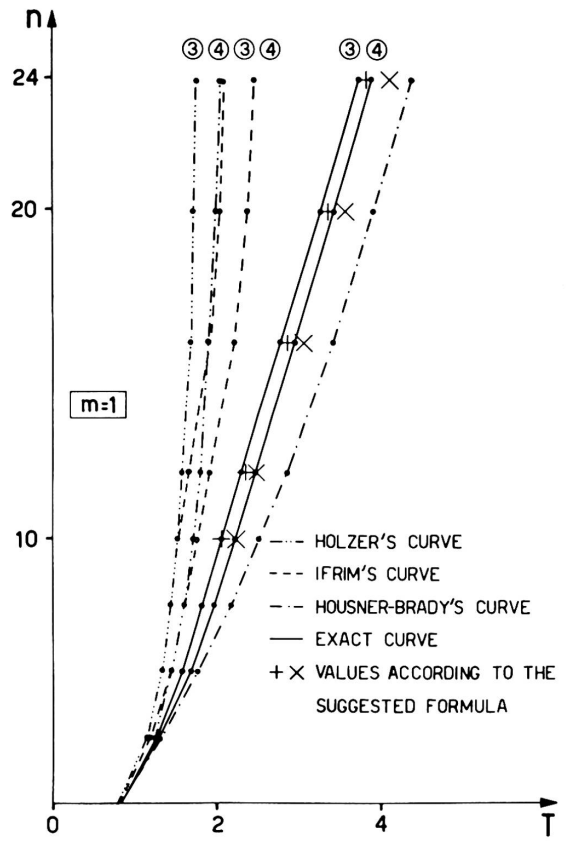
n
24
20
10
0
2
4
T
③④③④
③④
m=1
HOLZER'S CURVE
IFRIM'S CURVE
HOUSNER-BRADY'S CURVE
EXACT CURVE
+× VALUES ACCORDING TO THE SUGGESTED FORMULA

Fig. 4

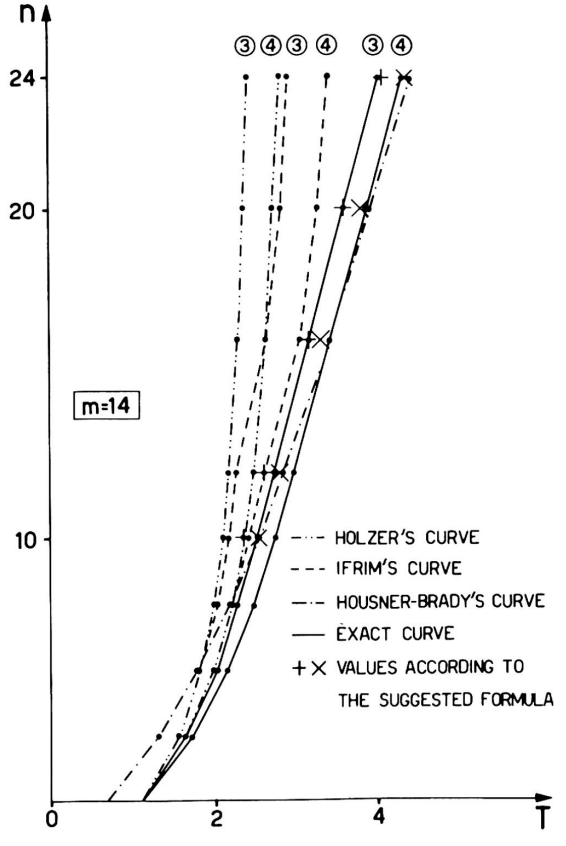
n
24
20
10
0
2
4
T
③④③④
③④
m=14
HOLZER'S CURVE
IFRIM'S CURVE
HOUSNER-BRADY'S CURVE
EXACT CURVE
+× VALUES ACCORDING TO THE SUGGESTED FORMULA

Fig. 5

Doing in this way it has been implicitely assumed that stiffners stiffness may change with joints rotation. Since this does not correspond to the real phenomenon it seems reasonable to introduce a reduction factor k. On the other hand since the ratio beams stiffness over columns stiffness increases with the number of spans, one may conclude that vibrations modes for multi-spanned frames usually exhibit smaller joints rotations. Therefore it can be predicted that factor k increases with the number of spans. Numerical results confirm this assumption giving values of k ranging from 0,65 and 1,00 for a number of spans between 1 and 14. The error is smaller than 20% also in limit cases.

In conclusion the following expression for the period of braced frames can be proposed:

$$T = 2\pi l_o^2 \sqrt{\frac{\mu_o}{E J_n}} \sqrt{\frac{m+1}{\frac{\sum J}{J_n} + \frac{e,n}{J_n}}} \kappa T'$$

2) - Space Structures

The problem of dynamics of space frames has been set up and analyzed in a second stage of studies.

The following fundamental hypotheses have been assumed:

a - linear elasticity of all members of structure;
b - infinite rigidity of each horizontal structure with regard to the deformations in the plane;
c - negligible torsional stiffness of resisting members of the structure.

Under these hypotheses for the generic space frame with in horizontal structures (such as the one shown in fig. 6) the dynamic deformed configuration is determined if the components:

$$u_i, \quad v_i, \quad \phi_i \qquad (i = 1,2 \ldots\ldots n)$$

for eabh horizontal structure are known. The u_i, v_i, ϕ_i correspond respectively to a rigid translation in the x direction, in the y direction and to a rigid rotation around the origin 0 of the i-th horizontal structure coinciding with its centroid.

The elastic response of the structure to a generic system of displacements and rotations given to each horizontal member can be represented therefore in the following form:

$$\begin{aligned}
X_j &= \sum_{i=1}^{n} A_{xx,ij}\, u_i + \sum_{i=1}^{n} A_{xy,ij}\, v_i + \sum_{i=1}^{n} A_{x\phi,ij}\, \phi_i \\
Y_j &= \sum_{i=1}^{n} A_{yx,ij}\, u_i + \sum_{i=1}^{n} A_{yy,ij}\, v_i + \sum_{i=1}^{n} A_{y\phi,ij}\, \phi_i \qquad (4) \\
M_j &= \sum_{i=1}^{n} A_{\phi x,ij}\, u_i + \sum_{i=1}^{n} A_{\phi y,ij}\, v_i + \sum_{i=1}^{n} A_{\phi\phi,ij}\, \phi_i
\end{aligned}$$

where X_j, Y_j, M_j are respectively the elastic reactions in the x and y direction and the torsional reaction around O arising at the level of the j-th horizontal structure. The coefficients A_{ij} represent the influence coefficients of the structure, i.e the elastic reactions at the j-th level due to displacements u_i, v_i, ϕ_i of the i-th level. They can be easily deduced if for each plane frame belonging to the space structure the reactions r_{ij} are known. Such reactions are due to the unit displacement of the generic i-th beam for all other beams prevented from translation.

In dynamics, if σ is the generic frequency of the structure in free vibrations, the displacements of the generic horizontal member turn out to be:

$$u_i = \bar{u}_i \sin \sigma t$$
$$v_i = \bar{v}_i \sin \sigma t$$
$$\phi_i = \bar{\phi}_i \sin \sigma t$$

Assumed that at each horizontal structure the mass is uniformely distributed, the inertial reactions in the x and y direction and the torsional reaction around O will be:

$$\bar{X}_j = - m_j \frac{d^2 u_j}{dt^2} = m_j \sigma^2 \bar{u}_j \sin \sigma t$$

$$\bar{Y}_j = - m_j \frac{d^2 v_j}{dt^2} = m_j \sigma^2 \bar{v}_j \sin \sigma t \qquad (5)$$

$$\bar{M}_j = - m_j \rho_j^2 \frac{d^2 \phi_j}{dt^2} = m_j \rho_j^2 \sigma^2 \bar{\phi}_j \sin \sigma t$$

where m_j is the total mass of the horizontal structure and ρ_j is the polar radius of giration of its area around O.

If columns masses are neglected, the equations of dynamic equilibrium are immediately obtained by equating (4) to (5). Setting the determinant of the coefficients of the system equal to zero one gets the algebraic equation of 3n degree in σ^2 whose roots σ_1^2, ... σ_n^2 allow the evaluation of the 3n free frequencies of the multi-story space structure.

It is obvious on the other hand that an iterative process is necessary if one wants to improve the values obtained by taking into account the mass of members. One should in fact recalculate the coefficients A_{ij} starting from the σ_i computed in the first cycle and taking into account the inertial forces of the beams and columns. Then the solution of the system of equations of dynamic equilibrium will lead to new values σ_i. The iteration process should be carried out as long as two consecutive solutions give almost the same value for the frequencies.

It should be born in mind, however, that in almost all cases the masses of horizontal structures are much larger that those ones of the columns. Consequently the values of σ_i given by the first iterative process are practically exact.

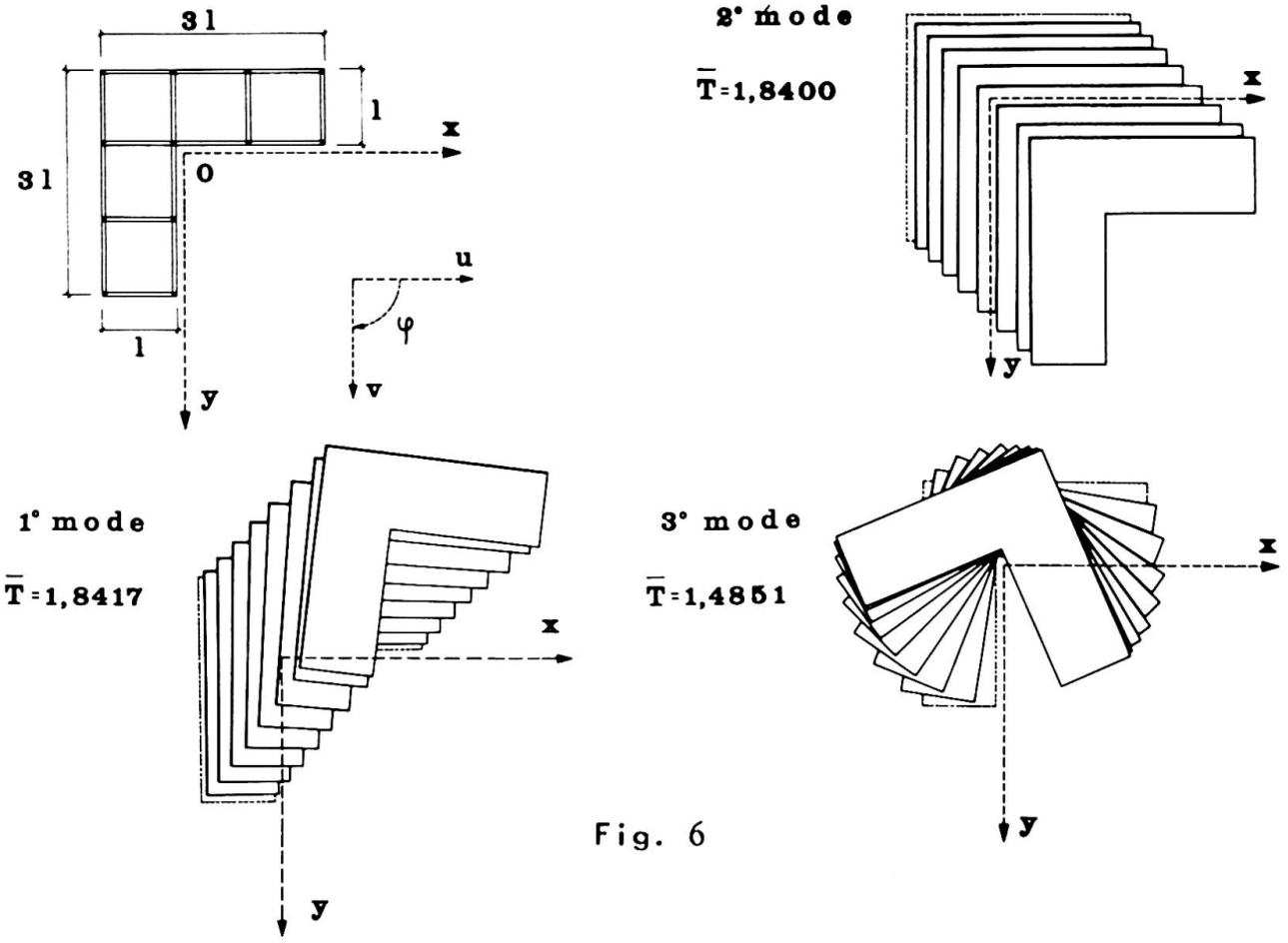
3l
l
x
0
3l
u
φ
l
y
v
2° mode
T̄=1,8400
x
y
1° mode
T̄=1,8417
x
y
3° mode
T̄=1,4851
x
y

Fig. 6

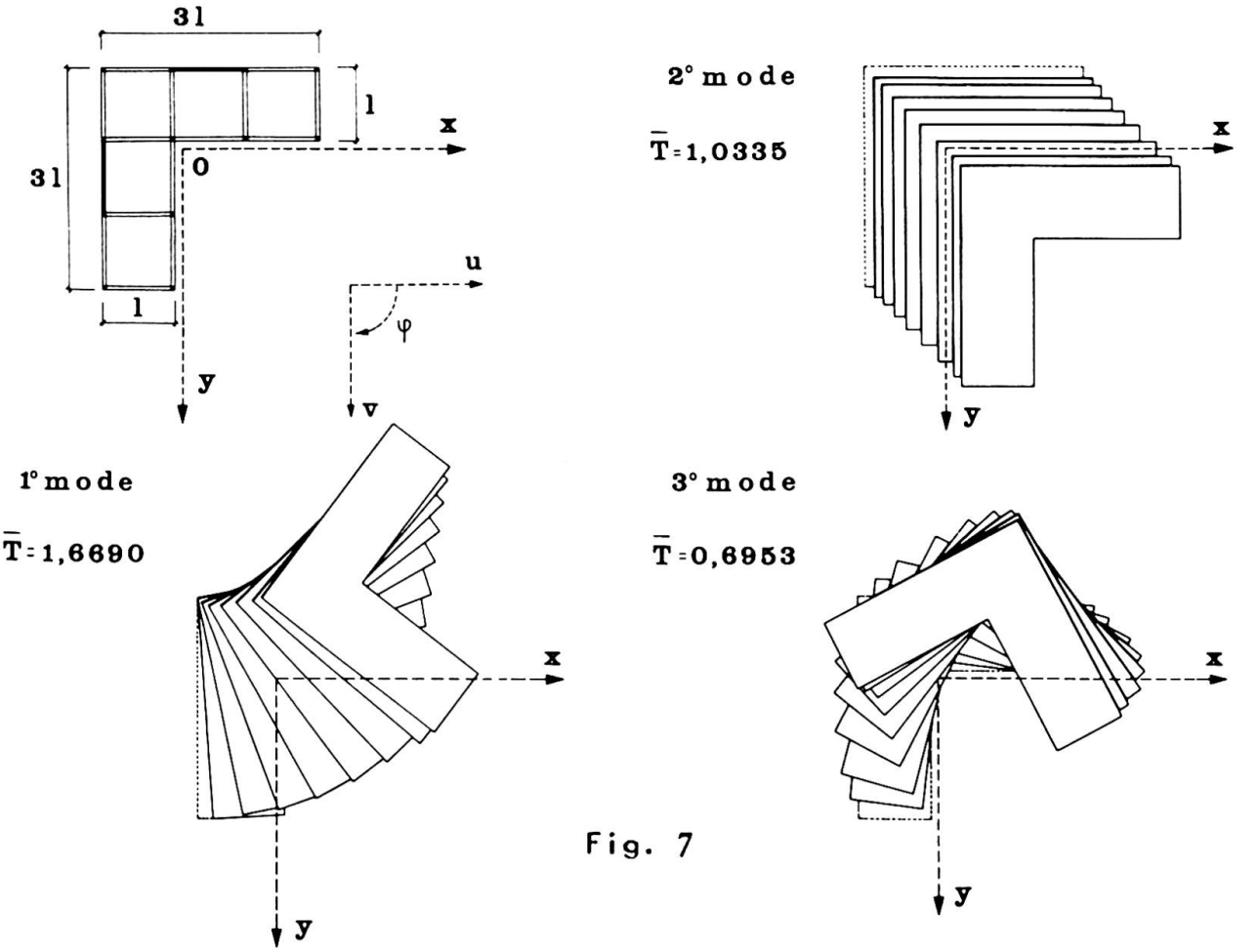
3l
l
x
0
3l
u
φ
l
y
v
2° mode
T̄=1,0335
x
y
1° mode
T̄=1,6690
x
y
3° mode
T̄=0,6953
x
y

Fig. 7

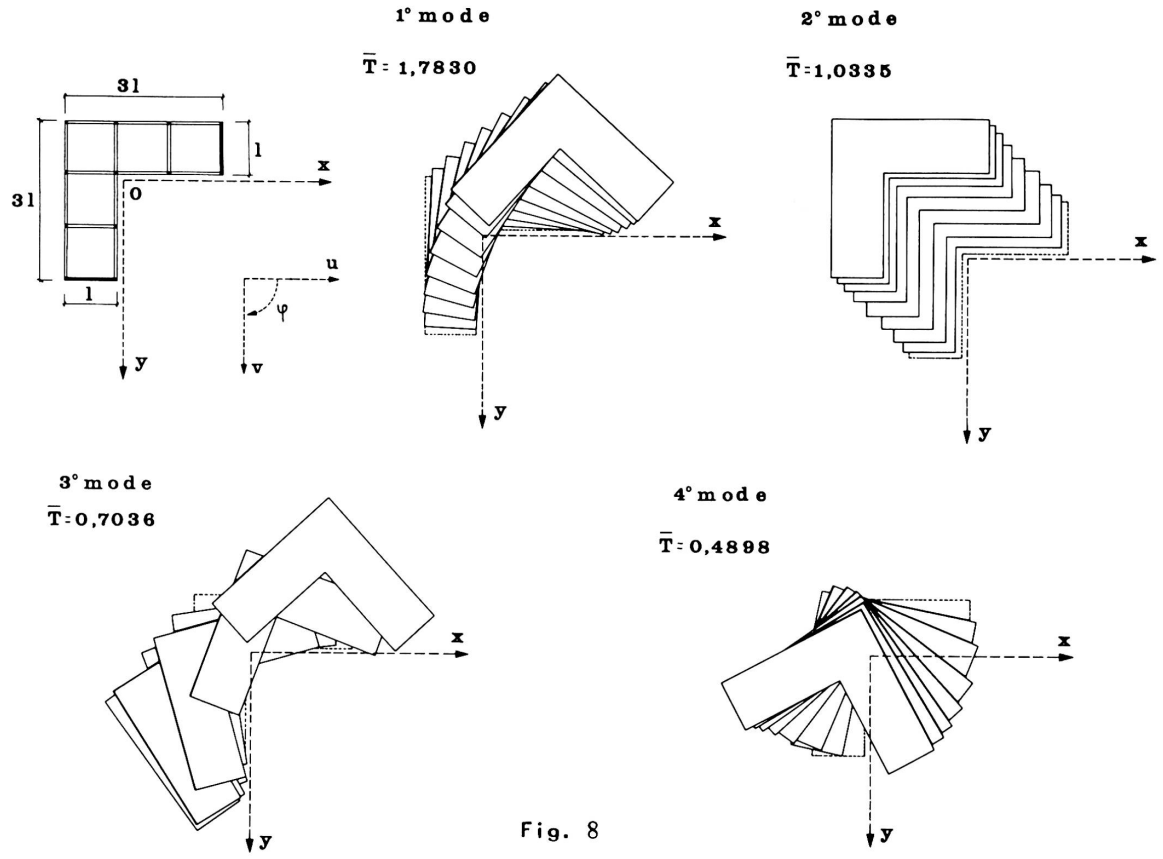
1° mode
$\bar{T}$ = 1,7830
2° mode
$\bar{T}$=1,0335
3° mode
$\bar{T}$=0,7036
4° mode
$\bar{T}$=0,4898
3l
3l
l
l
0
x
y
u
v
φ

Fig. 8

The foregoing procedure has been applied to a steel building with L plan and eight horizontal structures and with two orders of mutually orthogonal frames.

Three structural schemes of the building have been considered: the first one without windbracing (fig.6) and the other two with windbracing arranged as shown in figs. 7 and 8.

The dynamic analysis of the three space schemes has been carried out with the computer.

In the graphs previously mentioned have been represented the modes of vibration of $\overline{T}$ related to the period T by:

$$\overline{T} = \frac{T}{\sqrt{\frac{M_o \, l_o^3}{E \, J_n}}}$$

A comparison has been made between the results obtained in this way and the other ones given by decomposing the space structure in plane frames.

It can be concluded that the period of vibration obtained in the hypotheses of plane behaviour is usually smaller than the real value.

SUMMARY

It is briefly reported on the works of the Commission XIII of the Convention of European Constructional Steelwork Associations concerning the recommendations for designing steel structures in seismic area. The results of a study on the dynamic behaviour of plane and space framed structures are also shown. Finally some simplified formulae obtained through a large numerical investigation are suggested.

RÉSUMÉ

L'article résume très brièvement les travaux de la Commission de la Convention Européenne des Associations de la Construction Métallique, concernant les recommandations pour le calcul des bâtiment dans les zones seismiques. On expose aussi les résultats d'une étude sur le comportement dynamique de structures en portique dans l'espace. On donne l'expression de formules simplifiés pour le calcul de la période de vibration.

ZUSAMMENFASSUNG

Es wird ein kurzer Abriss von der Arbeit der Kommission XIII der Europäischen Konvention der Stahlbauverbände gegeben bezüglich der Empfehlungen zur Bemessung von Stahlbauten in Erdbebengebieten. Ebenso wird eine Studie über das dynamische Verhalten ebener und räumlicher Rahmentragwerke aufgezeigt. Schliesslich werden einige vereinfachte, durch erweiterte numerische Nachforschungen erzielte Formeln für die Schwingungsdauer angegeben.

Leere Seite
Blank page
Page vide

Factors affecting Response of Buildings to Wind and their Experimental Determination

Eléments ayant une influence sur la réponse d'édifices aux vents et leur détermination expérimentale

Faktoren, die die Reaktion von Gebäuden auf Windbelastungen beeinflussen und ihre experimentelle Bestimmung

SEAN MACKEY
Taikoo Professor of Engineering
University of Hong Kong

Wind action on buildings and structures has both static and dynamic effects. The static effects are primarily concerned with steady displacements obtained from steady forces and pressures resulting from time-averaged wind velocities. By custom, buildings have been designed to resist these effects. Dynamic effects, on the other hand are concerned with the tendency to set the structure oscillating. Increasing use of tall slender buildings with lightweight cladding and large column-free floor areas has forced engineers to pay much more attention to dynamic wind effects. Structural damping is a major factor which should be taken into account in this respect, since to decrease the resonant amplitudes of oscillation the dissipation of energy through structural damping must exceed the relevant energy inputs from the wind.

By applying the statistical theories used for communications technology the analysis of atmospheric turbulence is effected and its characteristics are represented by its energy spectra, its lateral correlation functions, and its probability distribution. Studies made to date, indicate that for heights up to that where the gradient winds prevail, variation in mean wind speed generally follows a power law profile, the exponent of which varies with ground roughness from about 0.15 for open unobstructed country to around 0.43 for heavily built-up urban centres, according to DAVENPORT [1] .

Investigations made by DAVENPORT [1] and SHIOTANI [2] show that the spectral density varies with the surface drag coefficient, which is a

function of the ground roughness. Except for some slight falling-off of energy with height, spectra obtained at different locations are more or less similar in shape and this has led DAVENPORT to suggest a universal type of formula:

$$\frac{n\ S(n)}{K\ \bar{V}^2} = C\ \frac{x^2}{(1+x^2)^{4/3}}$$

where n is the frequency; $\bar{V}$ is the mean wind speed; K is the drag coefficient; x is directly proportional to $\frac{n}{\bar{V}}$ and C is a constant.

Spatial correlation studies by the same investigators yield a spatial correlation coefficient, (i.e. $\sqrt{\text{coherence}}$), approximated by the exponential function:

$$R \propto e^{-\frac{\Delta S}{L}}$$

where Δs is the spatial separation and L is the scale of turbulence proposed by TAYLOR [3] . But in this respect, SINGER,[4] investigating radio masts, found the spatial correlation coefficient of similar wind components measured at different heights to be a function of the height ratio. Moreover, he found that within his range of interest cross spectra were essentially zero.

Apart from considerations of stability against time-averaged wind forces, the designer of tall buildings must also concern himself with the direct consequences to his structures of the fluctuating dynamic character of the wind. These include, inter alia, collapse of the structure due to peak load or fatigue; minor damage to the fabric, lift shafts, or partitions arising either from excessive deflexion or high local loading; and discomfort to the occupants caused by high sway accelerations.

Preferably, design factors should be simple and easy to apply. In this respect DAVENPORT'S simplified dynamic approach, using a gust factor G which takes into account the dynamic characteristics of the structure, has much to commend it. He suggests on expression for the wind pressure, p , at a point on the structure given by:

$$p = G\,\bar{p} = \left(1 + g\ r\ \sqrt{B + \frac{SF}{Y}}\right)\bar{p}$$

where:-

h = structure height

n_o = fundamental natural frequency of structure

T = time interval used for finding averages;
$\bar{V}$ = design velocity;
g = peak factor depending on n_o , and T ;
r = roughness factor depending on ground conditions and h ;
B = excitation from background turbulence, depending on h
S = scale factor depending on height/width ratio of structure n_o & $\bar{V}$
F = wave number at resonance = $n_o/\bar{V}$
γ = critical damping ratio;
$\frac{SF}{\gamma}$ = excitation due to resonant turbulence.

Essentially, these formulae predict the static equivalent load corresponding to the maximum deflexion. In applying them to natural gust loading, investigators have made several assumptions, including the following:

(i) wind is a stationary random process
(ii) variation of wind velocity with height follows a power law
(iii) velocity distribution is Gaussian in character
(iv) pressure coefficients are independent of frequency.

In order to assess correctly the effects of wind on a building it is necessary to know the spectrum of the wind; its spatial correlation, and the dynamic characterestics of the building. The dynamic characteristics include a knowledge of the natural frequency of the building and its damping. These are given by the following equations:

$$\frac{1}{\omega_r^2}[K]\{X^{(r)}\} = [M]\{X^{(r)}\}$$

$$\frac{1}{2\beta_r\omega_r}[C]\{X^{(r)}\} = [M]\{X^{(r)}\}$$

where the matrices $[K]$; $\{X^{(r)}\}$; $[M]$ and $[C]$ refer to the stiffness; the column mode shape; the mass and the damping, respectively. The results derived from application of these equations depends on the accuracy of determining the elements in $[K]$ and $[C]$. The elements in $[K]$ depend on the type of the structure and the properties of the materials used. Such factors as column and beam deformation; rotation of joints; floor and wall deformation; soil distortion and rigidity of foundations must be considered. Because of difficulties in obtaining experimentally the necessary information from full-scale buildings considerable reliance has had to be placed on mathematical models in order to evolve the methods of analysis now

available.

Correlation of model tests with the behaviour of full-scale buildings has been attempted by several investigators using three different types of approach. One of these, known as the resonance method, involves excitation of the building by means of a vibrator; the second makes use of run-down tests by pulling the building laterally and letting it go; the third relies on wind as the means of excitation, and a somewhat similar method developed by TANAKA [5] , involves measurement of minute vibrations excited by irregular forces such as microtremors and others

NIELSEN [6] has shown that decay tests can lead to overestimation of structural damping by several hundred percent, and he has succeeded in obtaining vibration characteristics of a 9-storey steel-framed building by steady-state tests. From the natural frequencies, damping and mode shapes obtained for several modes in this test he found the stiffness matrix giving the "best fit" to the modal properties determined experimentally. But NIELSEN'S experiment showed that any increase in the force level applied produced a corresponding increase in percentage damping and a slight decrease in resonance frequency. He also found for his building an additional mode of vibration, further to the normal modes, generated by the floor slabs vibrating laterally in phase as deep horizontal beams.

Similar investigations have been carried out by ENGLEKIRK & MATTHIESEN [7] on an 8-storey reinforced concrete building combining rectangular frames with shear walls, and by CRAWFORD & WARD [8] , using random wind excitation on a steel-framed building with a central concrete core. In the latter instance the natural periods were computed both for frame action only and for frame and core combined. The experimental results lie somewhere between the two values calculated and the ratios of the first three modes of vibration are not in agreement with the observed ratios. The investigators considered that this discrepancy resulted either from the fact that the window sections were not considered in calculating the shear stiffness and/or possible beam flexure and non-interaction of the core and structure. No measurements were taken simultaneously on the central core and on the framed structure to confirm this hypothesis.

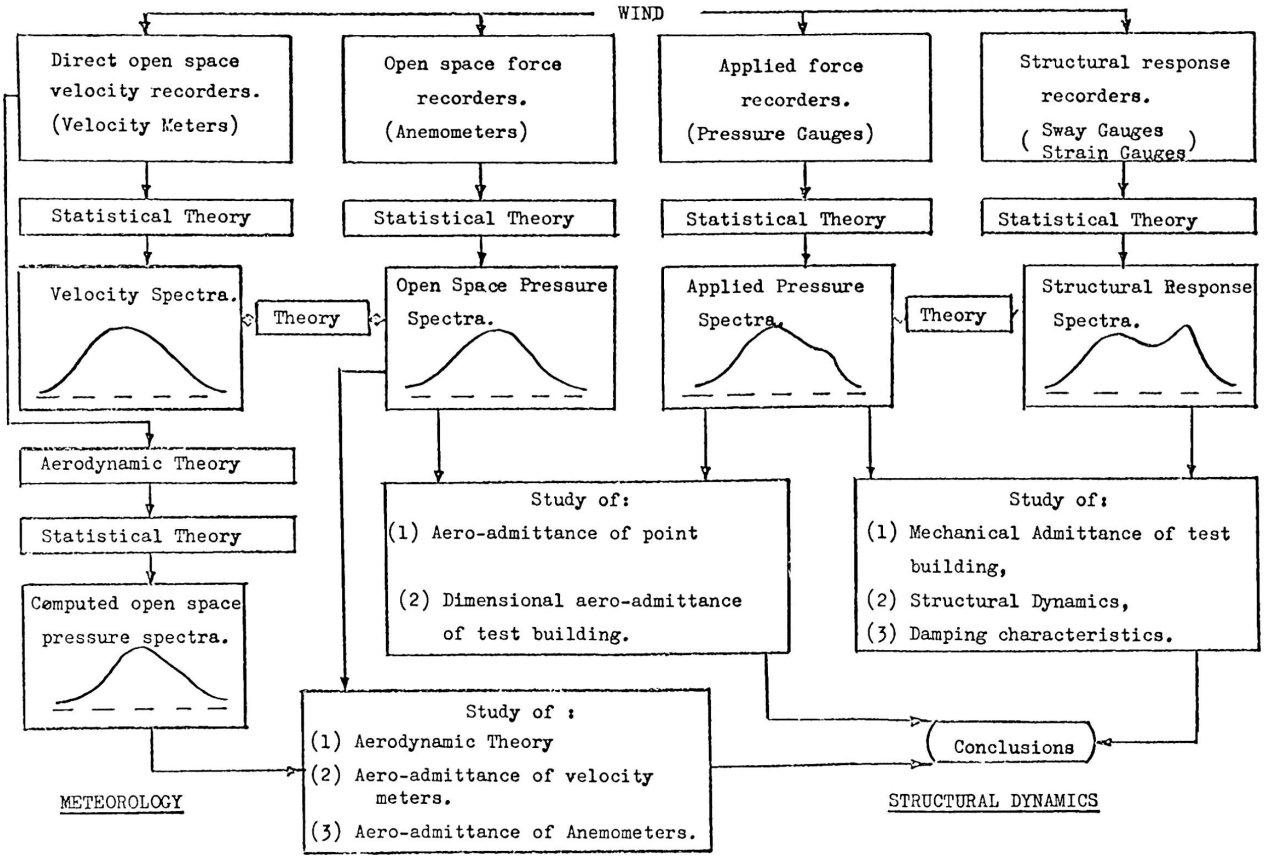

FIG. 1 - IDEALISED FLOW DIAGRAM FOR STUDY OF WIND EFFECTS ON STRUCTURES

The inadequacy of our present knowledge of these matters and the urgent need for comprehensive studies of natural winds and the response behaviour of full-scale structures under excitation from this cause are clearly demonstrated in the papers by BORGES [9] and by NEWMARK & HALL [10]. Such experiments are costly to execute and there is need for international collaboration in their planning to ensure that the results obtained from them are of real value, and cover both normal seasonal winds and those of typhoon magnitude.

An investigation, currently being undertaken at the University of Hong Kong is planned with this objective in mind. The nature of the investigation is diagrammatically set out in Fig. 1. but its scope must necessarily be limited initially, because of inadequacy of instruments for recording absolute wind velocities. In considering this figure it should be noted that a stationary statistical ergodic state is assumed and that the spectra referred to are vertically, horizontally and time-wise correlated.

It is anticipated that considerable difficulties will be experienced in determination of the aerodynamic admittance of the experimental building. Difficulties are also anticipated in determining, with sufficient accuracy, the actual patterns of wind-flow over the experimental site due to the limited funds available for instrumentation and site levelling.

In brief, the Hong Kong research involves construction of an experimental building on a low-lying exposed land area on the south-east coast of Hong Kong Island. The building is of fully-welded steel-framed construction with reinforced-concrete floors and glass curtain-wall cladding, so arranged that any part of the cladding may be disconnected temporarily from the structural frame. The building measures 60 ft. x 30 ft. in plan and ten-storeys or 100 ft. tall. It is so designed that it can be divided vertically into four sections, as shown in Fig. 2., each capable of acting independently of the others. Under high velocity winds the separate sections will be coupled together with shear connectors at every floor-level

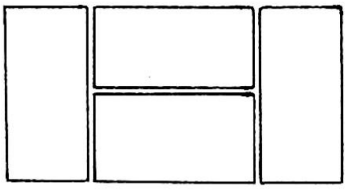

Fig. 2.

so that the whole building can act as a single monolithic unit. Uncoupled, the sections will be tested for sway under seasonal winds of moderate velocity. Dynamometers, installed across the vertical joints at various floor levels will record the drag effects of wind between the uncoupled sections.

Ahead and on one side of the building, approximately 200 ft. away from the nearest face two lines of free-standing latticed-steel masts, approximately 175 ft. tall, are being erected. Quick-response gust anemometers, designed by the Electrical Research Association of Great Britain, are attached to the masts in pairs at fixed height intervals. Collectively these anemometers, 60 in number, are being used to determine the wind spectra and the spatial correlation.

The pressure distribution over the faces of the building is being measured by 72 pressure gauges developed by the Building Research Station at Watford. The sway response of the building is to be recorded by Physitech Inc. electro-optical tracking instruments, which track the paths of targets attached to various points of the building.

The Benson-Lehner data logger installed accepts up to 240 channels of low-level analogue inputs in the range $\pm$ 10 mV to $\pm$ 500 mV full-scale deflexion, time multiplexes the data, makes an analogue-to-digital conversion, and records the binary or binary coded decimal equivalent on one-half inch wide, 9-track, magnetic tape. Operation of the system is illustrated in Fig. 3.

The analogue signals are sampled sequentially at the rate of 10 samples/second/channel by a reed relay multiplexer followed by a solid state submultiplexer which also performs the function of amplifying the low-level signals to $\pm$10 volts f.s.d. for maximum A-D converter resolution. No arithmetic is performed within the system, therefore all data indicated or recorded will be a function of the analogue signal level and amplifier gain. Identification data is included in the information recorded on the magnetic tape to provide the means of knowing which groups of channels have been selected for the scan sequence. This identification data also serves to identify the gain setting of the amplifier, as an individual amplifier gain is permanently associated with a particular channel group.

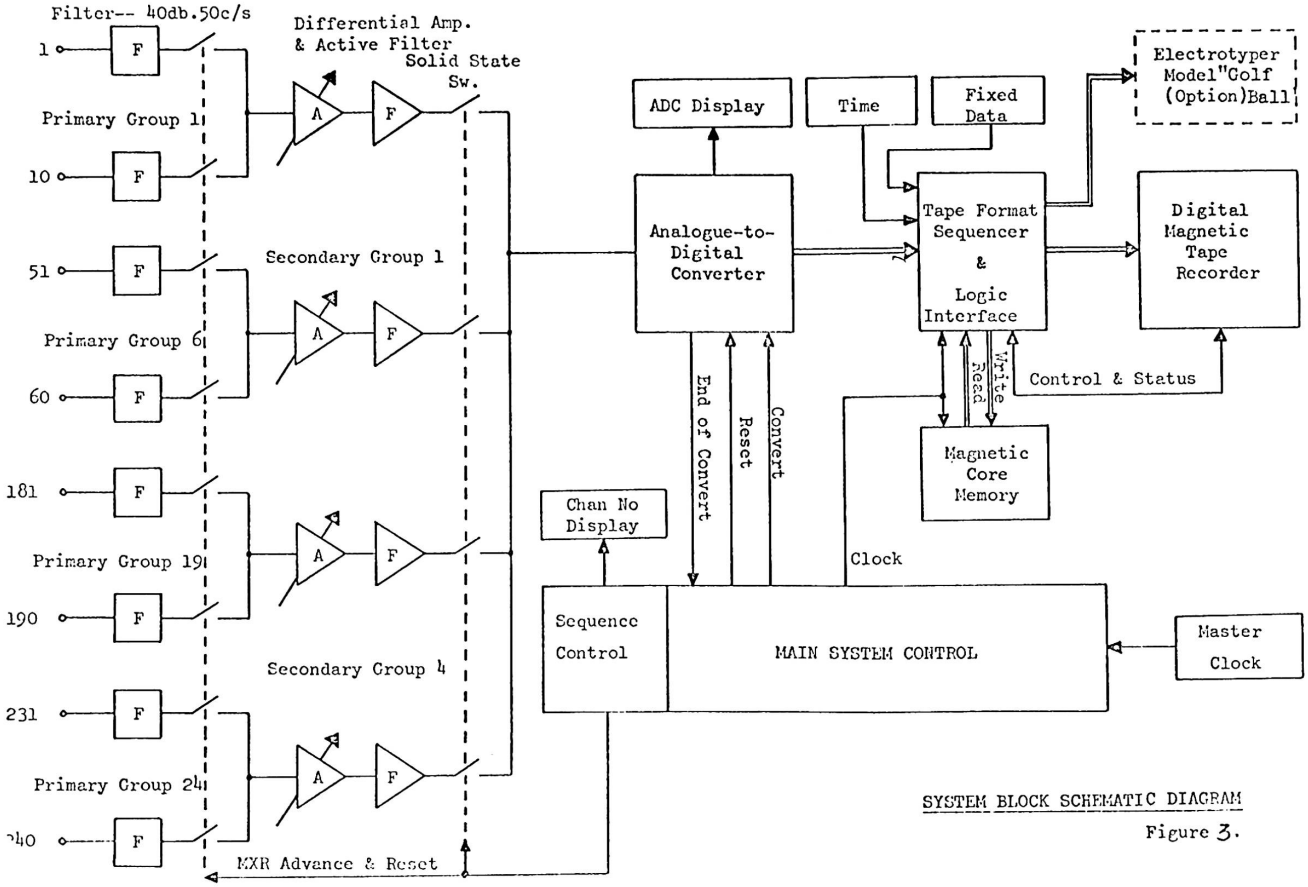

SYSTEM BLOCK SCHEMATIC DIAGRAM

Figure 3.

Analogue data is converted into a 9-bit binary two's complement digital format by the conventional method of successive approximation, each bit conversion occupying a time of 1.5 microseconds. The system accepts a continuous stream of data during the entire data acquisition and recording process, i.e. the scanning of the input channels is a continuous operation. Whilst interlock gaps are being generated on the magnetic tape, in accordance with IBM System/360 format requirements, digital data is stored in a buffer core store. The store is an AMPEX RF-2 of size 4096 words x 12 bits and, in operation, is made to resemble two independent stores of 2048 x 12. As one half of the store is being filled with digital data, the other half is unloaded at a transfer rate of 28,800 characters per second, via the tape format sequencer, to the digital magnetic tape unit.

The whole project is now nearing completion and recording is expected to commence in September of this year.

References

1. DAVENPORT, A.G. "The Relationship of Wind Structure to Wind Loading" Proc. Int. Conf. N.P.L. Lond. (1963)

2. SHIOTANI, M. "Lateral Structures of Gusts in High Winds" Phy. Sc. Lab. Nihon Univ. (1967)

3. TAYLOR, G.I. "Statistical Theory of Turbulence" Proc. Roy. Soc. A151 (1935): 156(1936)

4. SINGER, I.A. "Wind Gust Spectra" Ann. New York Acad. Sc. 116. Art.1. (1964)

5. TANAKA, T. "An Instrument for Brief Measurement of the Natural Period of a Building" Bull. Earthq. Res. Inst. 40 (1962)

6. NIELSEN, N.N. "Vibration Tests of a Nine-Storey Steel Frame Building" J. Engr. Mech. Div. ASCE. EMI. Proc. No.4660(1966)

7. ENGLEKIRK, R.E. & MATTHIESEN, R.B. "Forced Vibration of an Eight-Storey Reinforced Concrete Building" Bull. Seism. Soc. of Am. 57. (1967)

8. CRAWFORD, R. & WARD, H.S. "Determination of the Natural Periods of Buildings" Bull. Seism. Soc. of Am. 54 (1964)

9. BORGES, J.F. "Dynamic Loads"
Prel. Publ. I.A.B.S.E. 8th Congr. (1968)

10. NEWMARK, N.M. & HALL, W.J. "Dynamic Behaviour of Reinforced and Prestressed Concrete Buildings under Horizontal Forces and the Design of Joints"
Prel. Publ. I.A.B.S.E. 8th Congr. (1968)

SUMMARY

The response of a building to winds is governed by the meteorological data, the interaction of the wind and the building and the dynamic characteristics of the building. The available data is reviewed.

The author describes a project which will allow correlation of results from an experimental, 10-storey building with model results and existing code requirements. Wind velocities, pressure distributions over the building and the deflexion responses of the building will be measured.

RÉSUMÉ

La résistance au vent d'un bâtiment dépend des données météorologiques, de l'interaction du vent et de la construction, ainsi que de ses caractéristiques dynamiques. Les données connues sont revues ici. En plus, l'auteur décrit un projet qui permet de comparer les exigences des normes existantes avec les résultats d'un bâtiment d'essai de dix étages ainsi qu'avec les valeurs mesurées sur modèles réduits.

ZUSAMMENFASSUNG

Der Windwiderstand eines Gebäudes richtet sich nach den meteorologischen Gegebenheiten, nach der Wechselwirkung von Wind und Gebäude und nach den dynamischen Charakteristiken der Bauten. Diese Gegebenheiten werden berücksichtigt. Der Verfasser beschreibt ein Projekt, welches die Beziehung von Resultaten eines zehnstöckigen Gebäudes mit Modelergebnissen und bestehenden Norm-Anforderungen erlaubt. Gemessen werden die Windgeschwindigkeiten, Druckverteilungen über das Gebäude sowie die Ausbiegungen.

Behavior of Steel Frames Subjected to Repeated and Reversed Loads

Comportement des portiques multi-étagées en acier sous l'effet de charges répétitives et alternatives

Das Verhalten von Stahlrahmentragwerken unter Einfluß periodisch veränderlicher Wechsellasten

LAUREN D. CARPENTER
Instructor in Civil Engineering
Lehigh University
Bethlehem, Pennsylvania

LE-WU LU
Associate Professor of Civil Engineering
Lehigh University
Bethlehem, Pennsylvania

1) Introduction

Recent work in earthquake engineering has centered around full scale dynamic testing of multi-story buildings (Refs. 1 and 2) and computer studies of the behavior of simple systems under recorded earthquake motions or models thereof (Refs. 3, 4 and 5). Some tests have been performed to study the behavior of steel and concrete beams and frames under simulated wind, earthquake or impact loads. In recent tests at the University of California at Berkeley cantilever beams were tested under cyclic loads to study the behavior of these beams near the connecting zone (Refs. 6 and 7). In addition, as adjuncts to recent tests of multi-story frames at Lehigh University to study the static behavior under a monotonic load application, four frames were tested under a reversed loading after large inelastic deformations had occurred (Refs. 8 and 9). Currently available methods of analysis were found to adequately describe the static behavior of these test frames under the combined effect of gravity and monotonically increasing lateral loads. However, these methods were found to be inadequate to describe the static behavior of the frames under reversed loading even for relatively simple structures.

A research program has been initiated at Lehigh University in order to extend plastic design concepts to the design and analysis of structures subjected to seismic loadings. In the experimental portion of this program, two series of tests on single and multi-story frames were planned. This discussion gives a brief account of the first series of tests which has been completed recently.

2) Design of Test Frames

The test frames involved in the first series were designed to be typical of current aseismic design practice. The prototype frame was

an eight-story, single-bay structure. A bay width of 15 feet, story height of 10 feet and bent spacing of 18 feet were selected for the prototype frame shown in Fig. 1.

A three-story assemblage was designed to represent levels 5, 6 and 7 from the top of the building from which a single story frame representing level 7 was selected for the initial test. Half-story columns above level 5 and below level 7 were used to locate the point of inflection in the double curvature columns. The two frames in the first series are shown in Fig. 1 in their relative position with respect to the prototype frame.

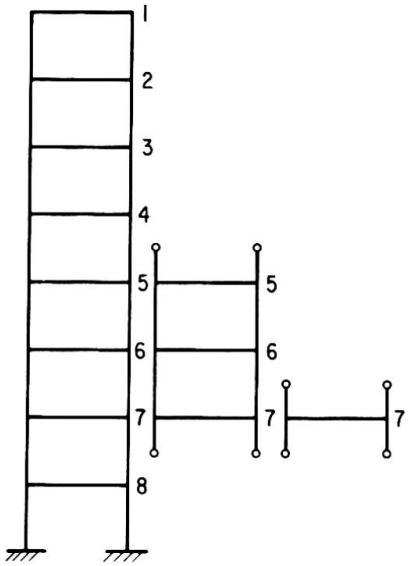

Fig. 1 Prototype Frame and Test Frames

The design and therefore the testing of the frame utilized a single horizontal load applied to the top of the assemblage. The frame was designed for constant story shear because for an eight-story frame the variation in the total aseismic design shear (Ref. 10) in the lower stories is usually small (Ref. 11). In addition, the envelope of maximum dynamic shear obtained from several modes of a shear type building has small variations in the lower portions of such a building (Ref. 12).

The gravity loadings used in the design were 80 psf full live load and 80 psf dead load on all the floors. An average live load reduction of 40% was used for both beams and columns. The working horizontal load was the summation of the design shears from the top of the structure down to and including the component at level 5. The working shear was equal to about 3½ percent of the sum of the dead loads through level 7.

The design also incorporated a ratio of column stiffness to beam stiffness which was selected to be representative of buildings designed using current aseismic design practice in California.

The plastic design method which was used to determine the members initially assumes no P-Δ effect and a likely-to-occur mechanism (Ref. 13). A plastic moment balancing analysis then was used to check that all moments are less than or equal to their fully plastic values. From the resulting moment diagram and sections required, the Δ's were calculated and the P-Δ moments were found. Redesign then included this P-Δ effect

and the sections required initially were altered when necessary.

Once the above set of members were selected, the frame was analyzed using the computer program (Ref. 14) described in the next section. By using this program repeatedly the members were selected such that they satisfied the requirements of aseismic design practice.

In summary, the three-story frame was designed and analyzed plastically and then checked by the allowable-stress method. The single-story frame was selected as a duplicate of the lower floor of this frame. The resulting member sizes selected were an 8WF40 section for the columns and a 10WF29 section for the beams. The member sizes and frame geometry for both frames are shown in Fig. 2.

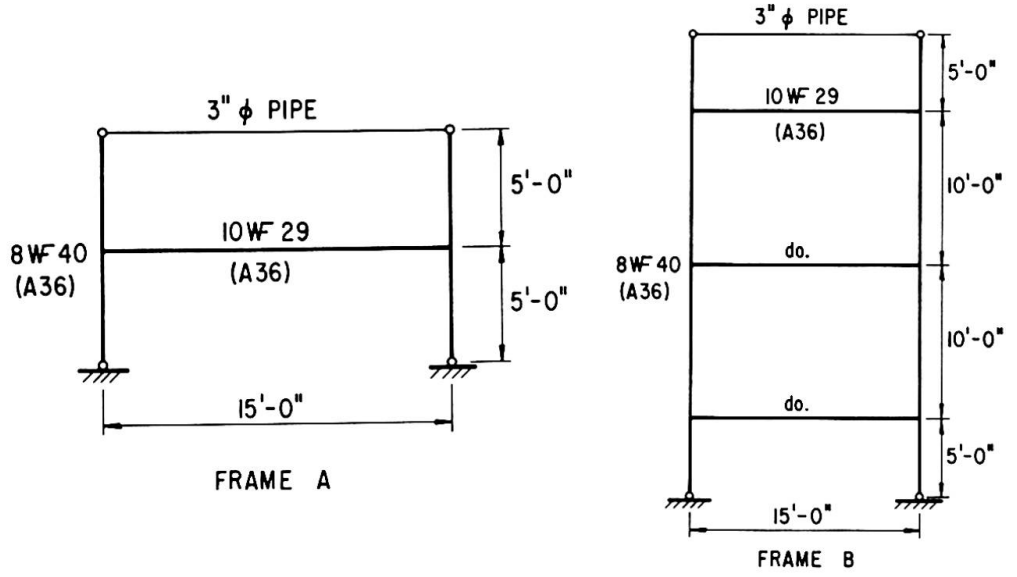

Fig. 2 Geometry and Member Sizes for Test Frames

3) Analyses of Test Frames

When the frames were analyzed under the combined earthquake and gravity loads, the change in member stiffness due to axial force, the overturning effects of the lateral load and the P-Δ moment were included.

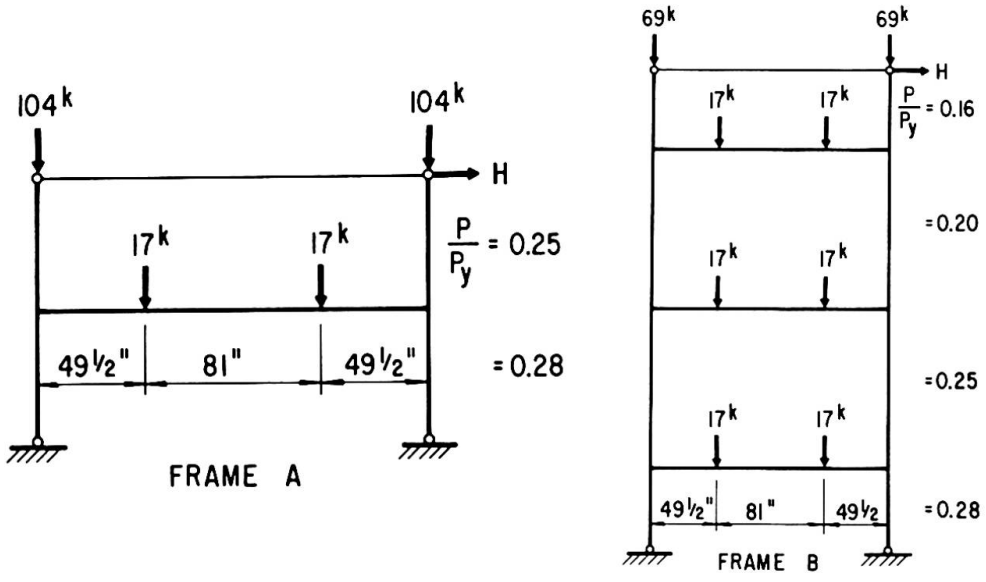

Fig. 3 Loads and Axial Load Ratios for Test Frames

At the working level of the monotonically applied horizontal load and the gravity loads shown in Fig. 3 the results of this second-order analysis were used to check the adequacy of the beams and columns with the AISC interaction formulas and satisfactory results were obtained. (In addition, the members of both frames were checked under the working level of gravity load only).

The analysis of each frame was then continued into the inelastic range past the point of frame instability. The load-deflection curves for both frames were essentially the same as shown in Figs. 4a and 4b.

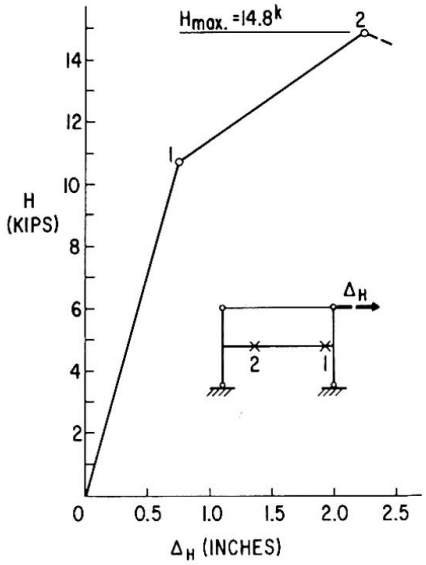

Fig. 4a Load-Deflection Curve for Frame A

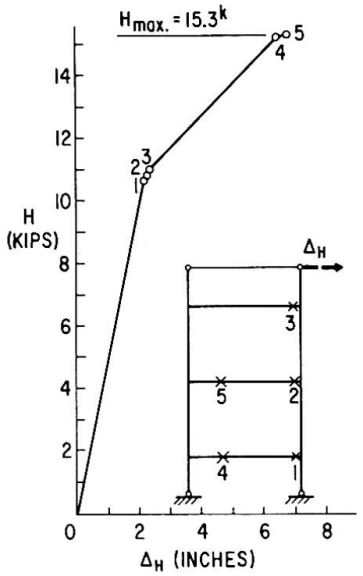

Fig. 4b Load Deflection Curve for Frame B

For the single-story frame the frame instability load and mechanism load coincide at a lateral load of 14.8 kips and at a deflection of 2.26 inches at the point of load application. However, the three-story frame became unstable at a load of 15.3 kips and a corresponding deflection of 6.83 inches before formation of a failure mechanism.

The single-story frame had a combined mechanism at its maximum load with the first hinge forming at the leeward end of the beam and the second hinge at the windward load point on the beam. The three-story frame had a similar pattern of hinge formation with the first hinge forming at a load of 10.7 kips in comparion to the working value of 5.2 kips. Since the ratio of maximum load to the working load is 2.9, a considerable savings could have been realized by utilizing more of the inelastic strength of the frame in design while keeping within acceptable drift limitations. In fact, a 13% lighter frame using 8W35 columns and 10W25 beams was analyzed under factored gravity plus lateral loads (L.F. = 1.30) (Ref. 13). The maximum load in this case was 8 kips which is considerably higher than the factored lateral load of 6.75 kips. However, for the former three-story frame which was designed for a lateral load of 3½ percent of total dead load, the ultimate value of lateral load is about 10 percent of the working dead load.

The above analyses were based on handbook values for cross-sectional properties and on the nominal static yield stress of 36 ksi specified for ASTM A-36 steel. The analyses were repeated after the cross-sectional shapes of the actual members used in the frames were measured and after the static yield stress levels were determined by testing tension specimens cut from adjacent pieces of the same length of steel. All material used was gag straightened by the producer.

4) Test Setup and Loading Program

The two frames were tested under constant (working) gravity loads and a program of statically applied cyclic horizontal displacements of the top of the frames similar to those used by E. P. Popov on the cantilever beams (Refs. 6 and 7).

Two unique devices were used to load and to brace the frames without offering any restraint to in-plane movements. Gravity-load simulators were used to apply the constant vertical loads to the quarter points of the beams through a spreader beam and to the column tops, and bracing linkages were used to prevent out-of-plane movements of the members of the frames (Ref. 15). The horizontal displacement was produced by mechanically displacing the top of the frame. Overall views of the test setups for the two frames are shown in Fig. 5.

Zero-moment end conditions were imposed on the ends of the columns at the assumed points of inflection above and below the main portions of each frame. Pinned-bases utilizing roller bearings were used at the lower end of each of the lower half-story columns. A pinned-end tie beam between the two ends of the top half-story columns was used. to distribute the horizontal force.

Displacements and rotations of various points throughout the frame were measured mechanically and electrically. Strain gages were used extensively throughout the structure. Computations from the strain gage readings and the measured deflections of the gaged points reduce the frames to determinate components.

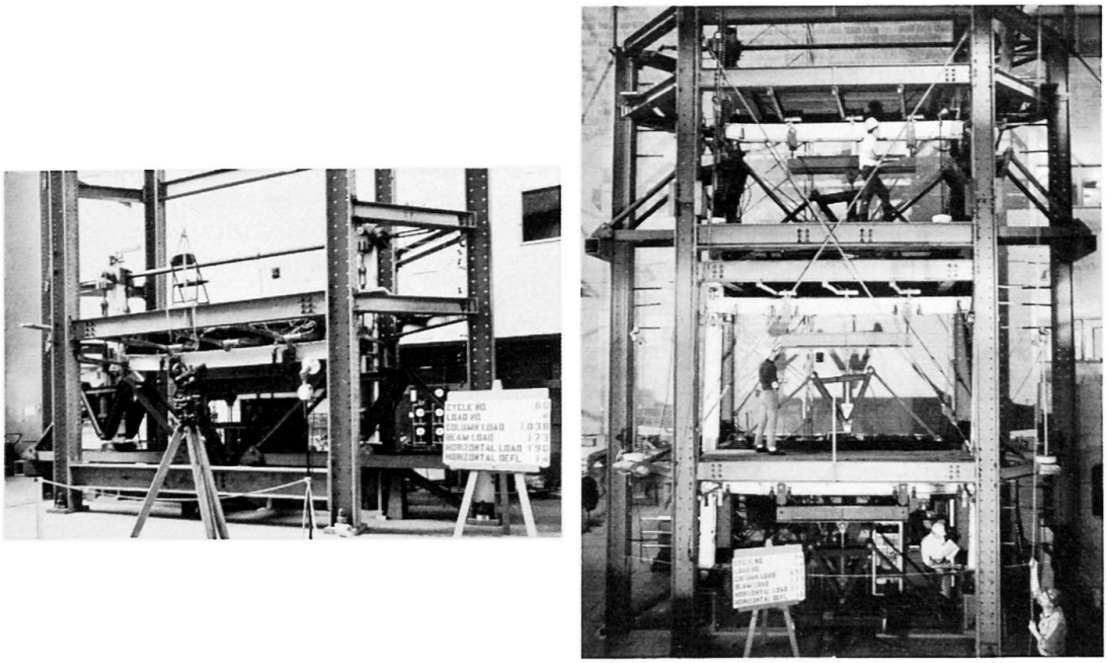

Fig. 5 Test Arrangements for Frame A and Frame B

Initially the gravity loads were applied to the frames and then sets of lateral displacements of increasing amplitudes were applied to the frames in a cyclic manner. In each case, the amplitudes to be cycled were selected to bracket the plastic hinge occurrences and other intermediate points on the respective load-deflection curves. For displacements in the elastic range three cycles were used at each amplitude and for inelastic range displacements five cycles were used. The number of replications at each amplitude was set to observe the stability of the hysteresis loops at the various amplitudes of deflection and inelastic conditions of the frames. The amplitudes selected for Frame A are superimposed on the load-deflection curve as shown in Fig. 6. The resulting displacements program is also given.

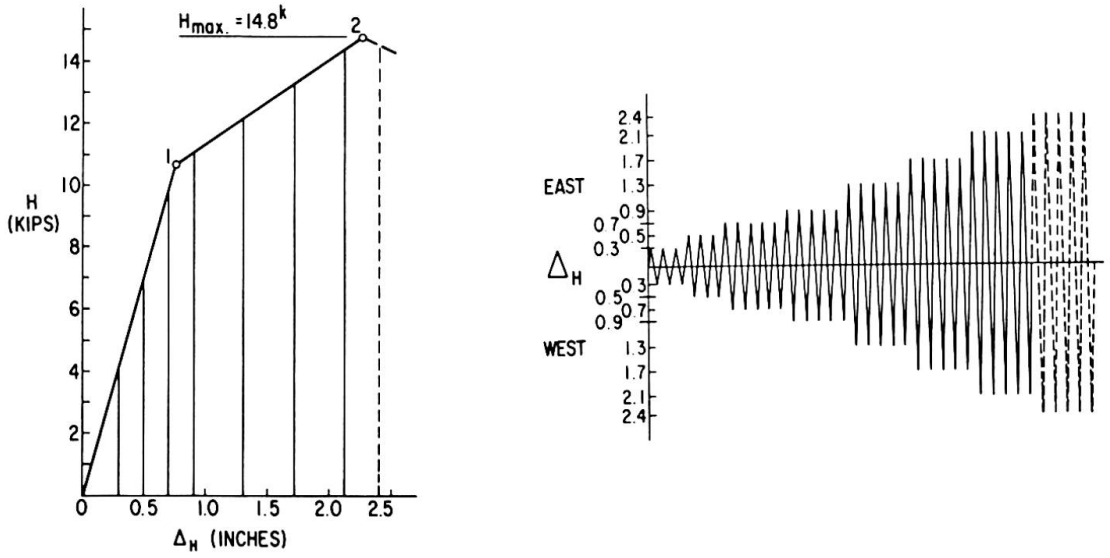

Fig. 6 Cycling Amplitudes and Horizontal Displacement Programs for Fram

During the tests, complete sets of static readings were taken at suitable intervals to permit construction of the hysteresis loops.

5) Test Results

Sixty cycles of horizontal displacement with increasing amplitudes were applied to the single-story frame with a maximum displacement of 5.2 inches which is 14 times the deflection at working load and 2.3 times the deflection at the maximum horizontal load. The three-story frame had 54 cycles at various amplitudes of displacement applied to it with a maximum cycled displacement of 10 inches. (At the end of the test 13.5 inches were applied in one direction). The displacement is 9 times the working load displacement and 1.5 times the deflection at the maximum predicted load. The ratios given above indicate the toughness and ductility of these steel frames. Cycles at selected amplitudes are shown in Fig. 7 for Frame B.

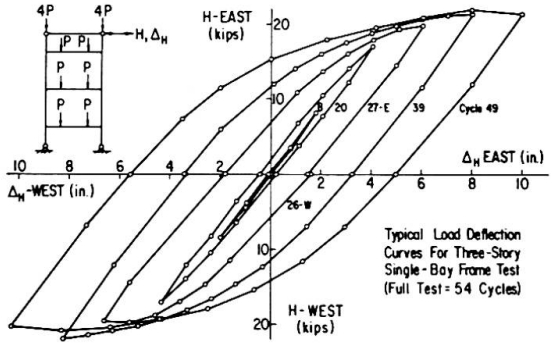

Fig. 7 Selected Load-Deflection Curves for Frame B

For the single-story frame the deflection at which the maximum load was reached was predicted closely by the monotonic analysis. But, for the three-story frame the maximum load occurred at a somewhat higher deflection (about 8 inches compared to the 6.8 inches predicted).

In addition, the replications of cycles at all amplitudes, even those beyond the frame instability deflection, showed stable results. This stability of the loops is indicated in Fig. 8 for the largest cycled amplitudes during the test of Frame A.

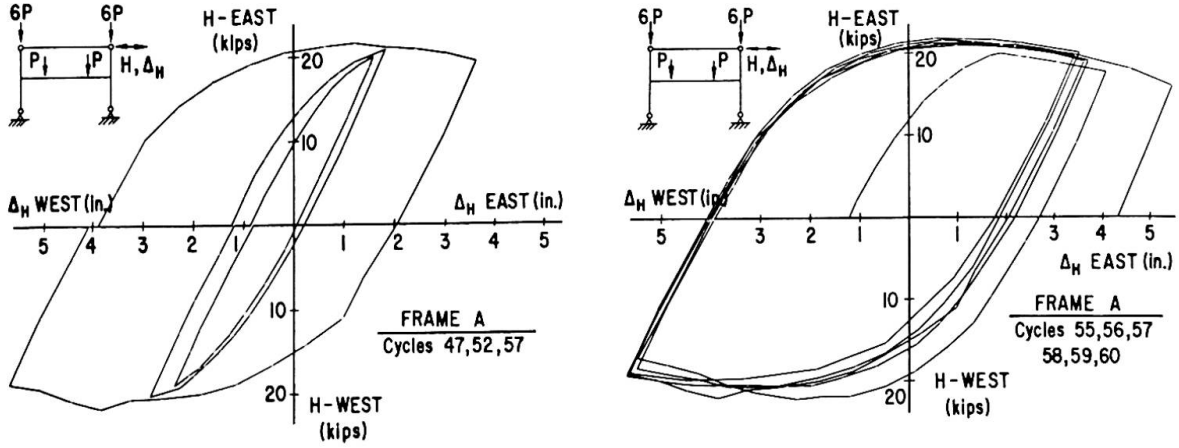

Fig. 8 Selected Load-Deflection Curves and Stability of Load-Deflection Curves for Frame A

Both tests showed a considerable reserve capacity for steel frames when subjected to cyclic lateral displacements. In each case, the maximum load the frame could withstand was about 40 percent greater than that predicted by the second-order elastic-plastic analysis of the frames under monotonically increasing lateral loads. (This percentage was computed after the analysis was redone with the actual experimental plastic moment values.)

One significant factor which tends to increase the lateral load over that predicted previously is the actual location of the plastic hinges in the beams. The analysis assumes no finite size for the beam-to-column connection whereas the yielding for the initial hinges was centered about one-half the depth of the beam from the column flange. Simple plastic analysis of Frame A shows a 17.5 percent increase in shear carrying capacity when the location of the first hinge is shifted as described above. (A preliminary estimate of the increase for a second-order analysis is 13 to 14 percent.)

The load-deflection behavior under reversed loading shows a higher maximum load than given by the monotonic analysis. However, this monotonic analysis agrees with the experimental results of the previous frame tests when the actual locations of the plastic hinges are considered. Therefore, this significant increase in maximum load is mainly due to the residual P-Δ moments existing in the frame when the reversed loading begins.

In addition, on each of the large cycles once the deflection at the maximum load had been exceeded the load carrying capacity dropped off much slower than the monotonic analysis indicated. For the monotonic analysis this downward slope is about 3 kips/inch, whereas the experimental curve showed a slope of about 1 kip/inch. This latter effect is mainly due to strain-hardening of the steel in the plastic hinge locations.

6) Conclusions

The following tentative conclusions may be drawn from the preliminary results presented in this paper:

1. The hysteresis loops are very stable even for deformations greater than those corresponding to the maximum lateral load.
2. A considerable increase in lateral load carrying capacity over that expected from a monotonic analysis is possible.
3. Strain-hardening plays an important role in the behavior of the frames for displacements greater than those at the maximum load.
4. The presence of the residual P-Δ moments has significant effects on frame behavior and must be included in developing a rational method of analysis for repeatedly loaded frames.

References

1. Nielson, N. N.
Vibration Tests of a Nine-Story Steel Frame Building, Journal of the Engineering Mechanics Division, ASCE, Vol. 92, No. EM1, Proc. Paper 4660, Feb., 1966, pp. 81-110.

2. Bouwkamp, J. G. and Clough, R. W.
Dynamic Properties of a Steel Frame Building, Steel Research for Construction, AISI, February, 1966.

3. Velestsos, A. S. and Newmark, N. M.
Effect of Inelastic Behavior on the Response of Simple Systems to Earthquake Motions, Proceedings of the Second World Conference on Earthquake Engineering, Vol. II, 1960, Japan, pp 895-912.

4. Berg, G. V.
A Study of the Earthquake Response of Inelastic Systems, Steel Research for Construction, AISI, February, 1966.

5. Goel, S. C.
Inelastic Behavior of Multi-Story Building Frames Subjected to Earthquake Motion, Ph.D Dissertation, University of Michigan, 1967.

6. Popov, E. P. and Franklin, H. A.
Steel Beam-to-Column Connections Subjected to Cyclically Reversed Loading, Steel Research for Construction, AISI, February, 1966.

7. Popov, E. P. amd Pinkney, R. B.
Behavior of Steel Building Connections Subjected to Repeated Inelastic Strain Reversal - Experimental Data - Report No. 67-31, University of California at Berkeley, December 1967.

8. Yarimci, E.
Incremental Inelastic Analysis of Framed Structures and Some Experimental Verifications, Ph.D. Dissertation, Lehigh University, 1966.

9. Arnold, P., Adams, P. F., and Lu, Le-Wu
The Effect of Instability on the Cyclic Behavior of a Frame, Fritz Laboratory Report No. 297.24, September, 1966.

10. Seismology Committee
Recommended Lateral Force Requirements
Structural Engineers Association of California, 1967.

11. Anderson, A. W , et al
Lateral Forces of Earthquake and Wind, Transactions, ASCE, Vol. 117, 1952, pp. 716-780.

12. Degenkolb, H. J.
Earthquake Forces on Tall Structures, Booklet 2028, Bethlehem Steel Corporation.

13. Driscoll, G. C., Jr., et al
Plastic Design of Multi-Story Frames, Fritz Laboratory Report No. 273.20, Summer, 1965

14. McNamee, B. M.
The General Behavior and Strength of Unbraced Multi-Story Frames Under Gravity Loading, Ph.D. Dissertation, Lehigh University, June 1967.

15. Yarimci, E., Yura, J. A., and Lu, Le-Wu
Techniques for Testing Structures Permitted to Sway, Experimental Mechanics, Society for Experimental Stress Analysis, Vol. 7, No. 8, Aug., 1967, pp. 76-84

Acknowledgments

The experimental study presented in this discussion forms part of a general investigation on "Behavior of Steel Frames Subjected to Repeated Loading" being carried out at Fritz Engineering Laboratory, Lehigh University, under the sponsorship of the American Iron and Steel Institute. Technical guidance is provided by a special Task Force organized by the Institute whose membership includes: I. M. Viest (chairman), G. V. Berg, H. J. Degenkolb, G. C. Driscoll, Jr., T. V. Galambos, C. W. Pinkham, E. P. Popov and J. L. Stratta. The authors would like to acknowledge the support given by the Institute and the advice received from the members of the Task Force.

SUMMARY

The experimental behavior of two steel (A36) frames, a single-story, single-bay frame and a three-story, single-bay frame, recently tested under constant gravity loads and a program of gradually increasing amplitudes of cyclic lateral displacement is summarized. The design and the second-order elastic-plastic analyses of the test frames under monotonically applied horizontal load are outlined and comparisons with experimental results are made.

RÉSUMÉ

Le comportement expérimental de deux portiques multi-étagés en acier A36 (Equivalent à Adx charpente), portique à un niveau et à une travée, et portique à trois niveaux et une travée, récemment testés pour des charges normales constantes et pour des déplacements cycliques latéraux dont les amplitudes ont été incrémentées graduellement, est resumé. Le calcul et les analyses du second ordre dans le domaine élasto-plastique des portiques sous charge horizontales unidirectionnelles, sont présentés, ainsi que le rapprochement avec les résultats expérimentaux.

ZUSAMMENFASSUNG

Das Verhalten eines einfachen Ein-Stockwerkrahmens und eines Drei-Stockwerkrahmens, beide mit der Stahlsorte A36 auseführt, wurde kuerzlich experimentell untersucht. Die Beanspruchung des Tragwerkes setzt sich zusammen aus vertikalen Kräften von konstanter Grösse (Graditationskräfte), und Kräften welche aus den veränderlichen, horizontalen Knotenverschiebungen resultieren. Die Konzeption der Versuchsanordnung sowie die elasto-plastischen Berechnungen zweiter Ordnung sind beschrieben und Vergleiche mit den experimentellen Resultaten wurden aufgestellt.

Performance of Steel Beams and Their Connections to Columns During Severe Cyclic Loading

Comportement de poutres en acier et de leur assemblage sur colonnes sous d'importantes charges périodiques

Das Verhalten von Stahlträgern und ihren Anschlüssen an Stützen unter schweren zyklischen Belastungen

E.P. POPOV
Professor of Civil Engineering
University of California, Berkeley

Introduction

In the Preliminary Publication for the 1968 IABSE Eighth Congress, D. Sfintesco makes reference to some of the earlier work at the University of California on steel beam-to-column connections subjected to repeated and reversed loading (1, 2). It is the purpose of this discussion to call attention to further published results (3, 4) and to provide the readers with a summary on the new work which should shortly become generally available in print (5, 6). It is gratifying that the earlier analyses as well as the penetrating opinions and observations by D. Sfintesco expressed in the Preliminary Publication are in essential agreement with the later findings.

Conventional stationary structures such as buildings, bridges and towers are not immune to dynamic loadings. As pointed out by J. Ferry Borges in the Preliminary Publication, such loadings are associated with wind and earthquake, as well as machinery, traffic, and blast loads. The general effect on stationary structures due to such loads is essentially analogous. However, the loading of buildings caused by strong earthquakes is particularly severe.

During an earthquake the soil on which a building is situated becomes subjected to a rapid back-and-forth motion in horizontal and vertical directions. The horizontal motion usually causes the more damaging effect. A representative accelerogram for a horizontal movement for an earthquake (7) is shown in Fig. 1. The typical rapidly varying inputs at the ground level reflect themselves in relatively slow swaying motions of buildings. This is due to the fortunate lack of resonance between the frequency of the ground motion input and the natural period of vibration of typical high-rise buildings.

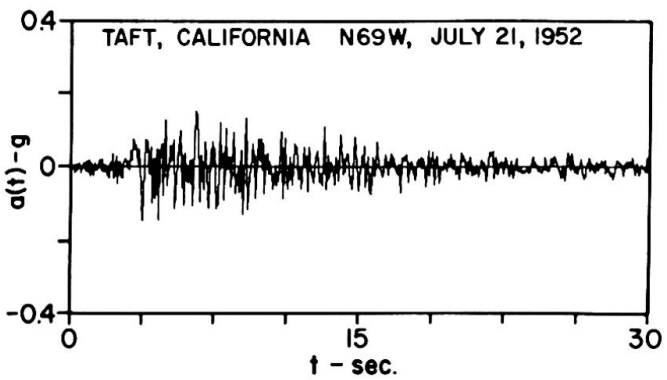

Fig. 1

The swaying motion of a severely strained building is shown schematically in Figs. 2(a) and (b), where it is assumed that the columns are relatively inflexible. This is in conformity with the current design practice which permits essentially only elastic action in the column, but allows substantial inelastic deformation in the beams and their connections to the columns.

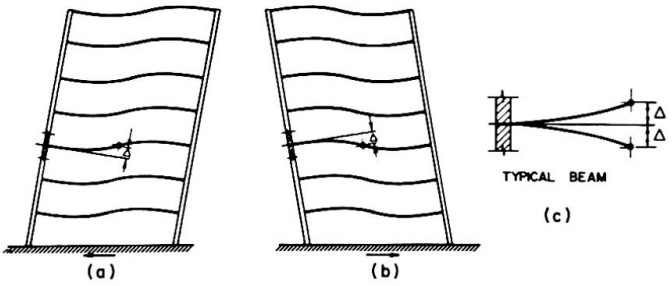

BEHAVIOR OF A FRAME IN AN EARTHQUAKE

Fig. 2

On the above basis all specimens for the first series of the California experiments were so designed that yielding occurred in the beams and their connections and not in the columns. Such yielding of the members provides damping of the structure and assures dissipation of the energy input due to an external cause such as an earthquake.

In the specimens designed for this series of experiments no attempt was made to simulate gravity loading. The question of simulating more accurately the loading on actual beams, as well as of permitting columns to exhibit some controlled yielding, is the subject of a current investigation (8).

Details of Specimens

The specimens selected in the first series of the California tests resembled the isolated element of a building frame shown in Fig. 2(c). The details of the specimens are shown in Figs. 3, 4, 5, and 6. In the specimens of the F1 type, Fig. 3, the beam was directly welded to the column stub. In the specimen of the F2 type, Fig. 4, welded connecting plates were used. In the specimen of the F3 type, Fig. 5, the attachment of the beam to the column stub through the connecting plates was achieved using high-strength bolts. The welded detail W1 for connecting a beam to the web of the column is shown in Fig. 6. All of these details represent the types widely used in the construction of steel buildings.

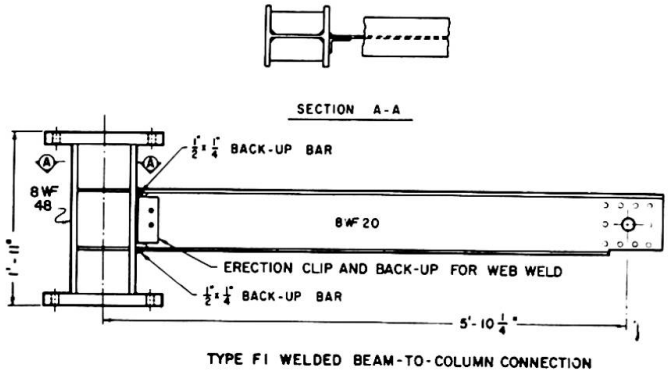

TYPE F1 WELDED BEAM-TO-COLUMN CONNECTION

Fig. 3

In several of the specimens of the F2 and the F3 types the thickness of the connecting plates was varied. For two web connected specimens, designated as W2, the connecting plates were tapered or shaped to provide a more gradual change in the cross-section of the beam flange. A total of twenty specimens using A-36 steel were fabricated according to above details. Four additional specimens, two of the F1 type and two of the F2 type, using A-441 steel formed a part of the same series of experiments (4, 5). The specimens made of a higher strength steel are identified by letters HS and referred to as F1HS and F2HS.

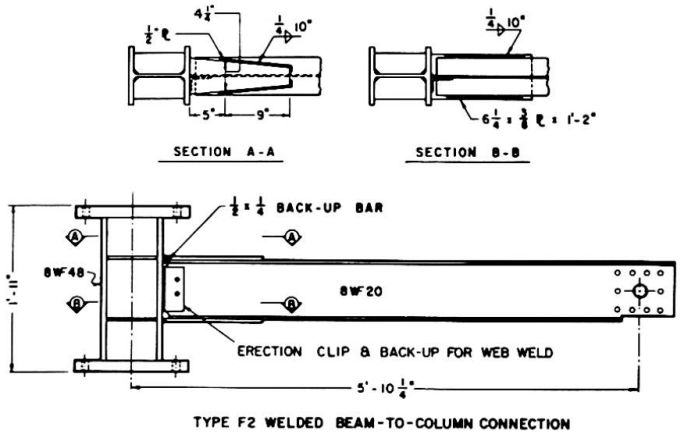

TYPE F2 WELDED BEAM-TO-COLUMN CONNECTION

Fig. 4

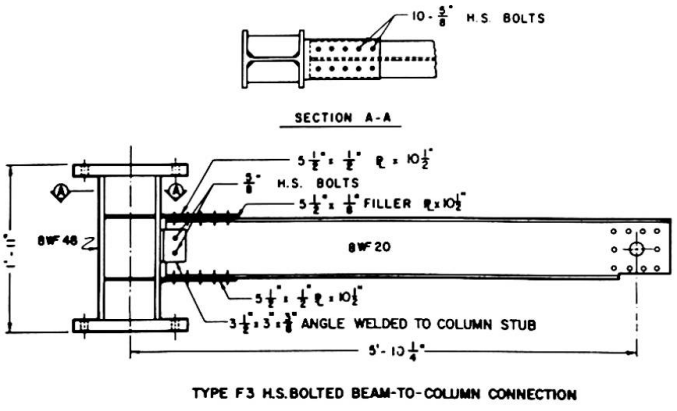

TYPE F3 H.S.BOLTED BEAM-TO-COLUMN CONNECTION

Fig. 5

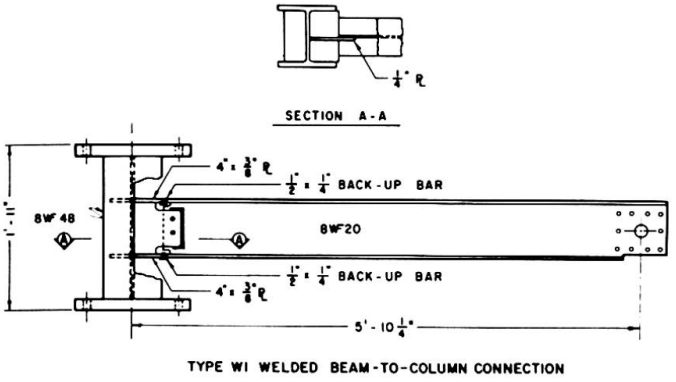

TYPE WI WELDED BEAM-TO-COLUMN CONNECTION

Fig. 6

Experimental Procedure

The basic experimental set-up is shown in the photograph of Fig. 7. A double acting hydraulic cylinder provided the desired load input at the tip of the cantilever. Experiments were controlled either by a strain gage near the built-in end of the cantilever, or by a selected tip deflection. Some typical loading programs are shown in Fig. 8. A considerable variety of such programs was used in the experiments.

In Fig. 8(a) the step-ladder type of sequence for the tip deflection is shown. Here the displacement amplitudes are arbitarily increased gradually. An experiment with a few strong initial displacements followed by the step-ladder sequence of the tip deflection is shown in Fig. 8(b).

Numerous measurements were recorded during the experiments (4, 5). Among these the load-deflection characteristics of the beam are particularly important.

Principal Experimental Results

Applying repeated and reversed loading of the type shown in Fig. 8 causes considerable yielding in the specimens during each cycle of loading application. Therefore, as is to be expected, after a number of cycles the specimens fail. The manner of failure is strongly dependent on the type of specimen, whereas the number of cycles to failure depends on the amplitudes of the tip deflection. These results are summarized in Table 1. For a more complete description of the experiments and the results, the reader is referred to References 4 and 5.

TABLE I

Specimen	Cycles to Failure	Type of Cycling Number of Cycles at Given Tip Deflection*	Total Energy Absorption kip - in.
F1-C1	28	5 at ± 1 in.; 5 at ± 2 in.; 10 at ± 3 in.; 8 at ± 4 in.	-------
F1-C2	22 1/2	22½ at ± 3 in.	2,411
F1-C3	120	100 at ± 1 in.; 20 at ± 3 in.	3,734
F1-C4	39 1/2	20 at ± 2 in.; 19 1/2 at ± 3 in.	2,837
F1-C6	32	5 at ± 3/4 in.; 5 at ± 1 1/2 in.; 10 at ± 1 1/2 in. to ± 4 in.; 12 at ± 4 in.	2,574
F2-C1	18	5 at ± 1 in.; 5 at ± 1 1/2 in.; 8 at ± 3 in.	-------
F2-C4	44	42 at ± 1 1/2 in.; 2 at ± 2 in.	2,495
F2A-C7	38 1/2	15 at ± 3/4 in.; 15 at 1 1/4 in.; 8 1/2 at ± 1 3/4 in.	1,054
F2B-C8	32 1/2	15 at ± 3/4 in.; 15 at ± 1 1/4 in.; 2 1/2 at ± 1 3/4 in.	533
F3-C1	9 1/2	5 at ± 2 1/2 in.; 4 1/2 at ± 4 in.	-------
F3-C5	30	30 at approximately ± 2 1/2 in.	1,533
F3A-C7	65 1/2	15 at ± 3/4 in.; 15 at ± 1 1/4 in.; 15 at ± 1 3/4 in.; 15 at ± 2 1/4 in.; 5 1/2 at ± 3 in.	2,488
F3B-C7	33 1/2	15 at ± 3/4 in.; 15 at ± 1 1/4 in.; 3 1/2 at ± 1 3/4 in.	704
W1-C7 **	37	15 at ± 3/4 in.; 15 at ± 1 1/4 in.; 7 at ± 2 in.	926
W1-C9	51 1/2	2 at ± 1 3/4 in.; 15 at ± 3/4 in.; 15 at ± 1 1/4 in.; 15 at ± 1 3/4 in.; 4 1/2 at ± 2 1/4 in.	1,500
W2A-C7	46 1/2	15 at ± 3/4 in.; 15 at ± 1 1/4 in.; 15 at ± 1 3/4 in.; 1 1/2 at ± 2 1/4 in.	1,189
W2B-C10	30	5 at ± 1 3/4 in.; 15 at ± 3/4 in.; 10 at ± 1 1/4 in.	651
F1HS-C7	74	15 at ± 3/4 in.; 15 at ± 1 1/4 in.; 15 at ± 1 3/4 in.; 15 at ± 2 1/4 in.; 14 at ± 2 3/4 in.	3,597
F1HS-C11	73	5 at ± 2 1/4 in.; 15 at ± 3/4 in.; 15 at ± 1 1/4 in.; 15 at ± 1 3/4 in.; 15 at ± 2 1/4 in.; 8 at ± 2 3/4 in.	3,539
F2HS-C7	35 1/2	15 at ± 3/4 in.; 15 at ± 1 1/4 in.; 5 1/2 at ± 1 3/4 in.	897
F2HS-C9	54 1/2	2 at ± 1 3/4 in.; 15 at ± 3/4 in.; 15 at ± 1 1/4 in.; 15 at ± 1 3/4 in.; 7 1/2 at ± 2 1/4 in.	2,149

* Tip deflections are approximate, and are measured from mean position.
** Results from two defectively fabricated W1 specimens are not included.

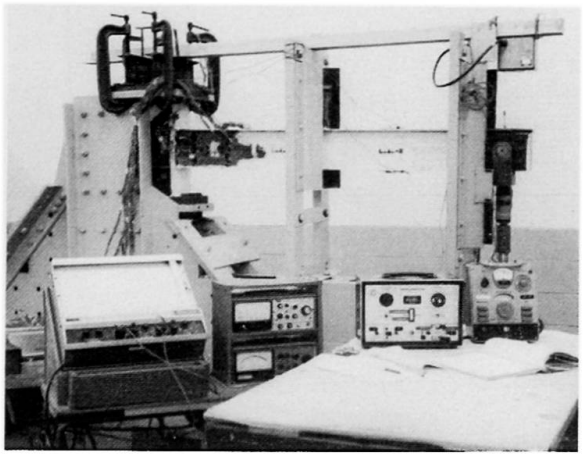

Fig. 7

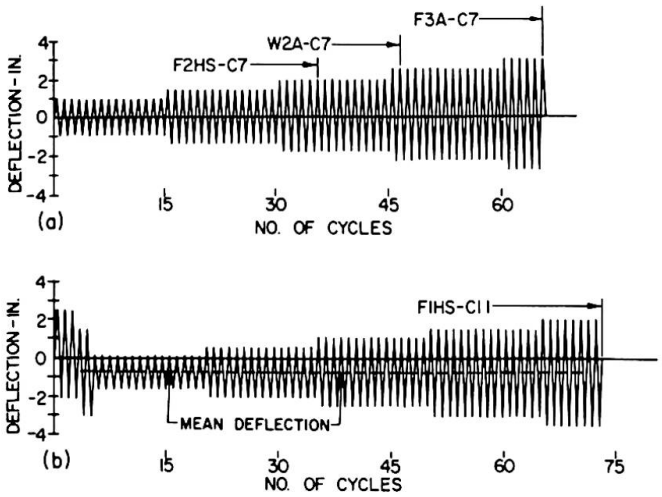

Fig. 8

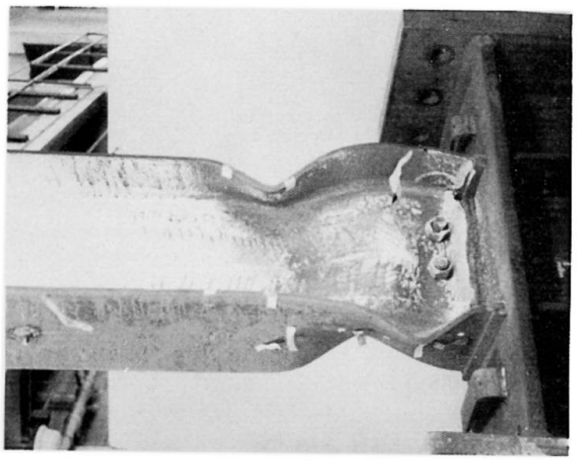

Fig. 9

A few photographs showing the manner of the ultimate failure of specimens are reproduced in Fig. 9, 10 and 11. Although such information is significant, one does not design for this condition to occur, and it is more important to answer the following two questions:

1. Can steel beams and their connections to columns withstand a sufficient number of cycles of large amplitude, i.e. of load reversals causing severe plastic strains, without breaking during a major earthquake?

2. How dependable is the energy absorption capacity per cycle during severe straining of steel?

An examination of Table 1, bearing in mind the exceptional severity of the imposed strains in the reported experiments, provides an affirmative answer to the first question. With the exception of two defectively fabricated specimens, for each specimen the number of cycles before failure occured was quite large in relation to what might be anticipated during a severe earthquake.

An examination of the hysteresis loops is necessary to answer the second question. Three sequences of hysteretic loops from one of the experiments are shown in Fig. 12. Their remarkable repetitivness and reproductibility during a number of consecutive identical cycles is noteworthy. Experimental evidence also clearly demonstrates that the onset of flange buckling does not cause the capacity of the beam to deteriorate significantly. The gradual work-softening which may be noted from Fig. 12 appears to be of no importance in seismic design as it occurs only after an excessively large number of load reversals.

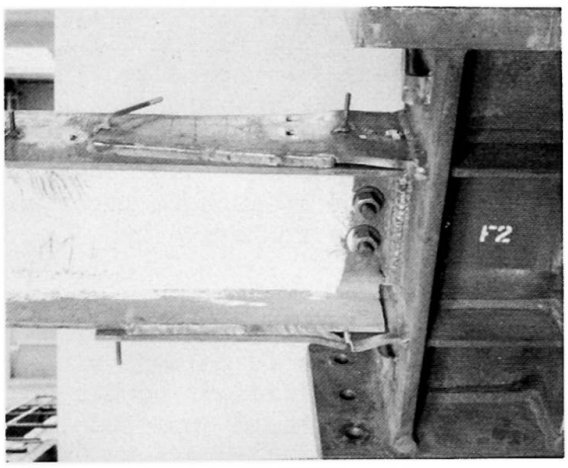

Fig. 10

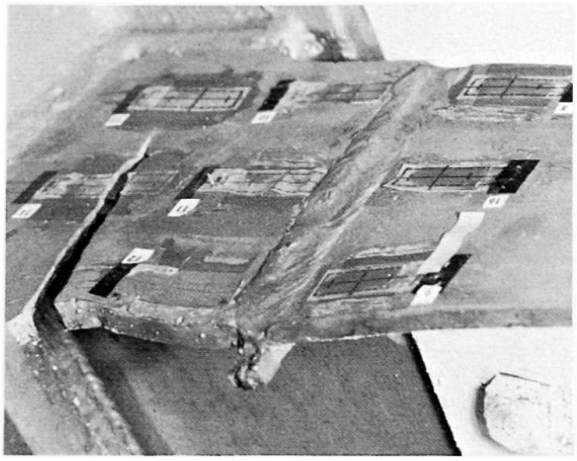

Fig. 11

The completed experiments further provided good evidence on the increase in the size of the hysteresis loops with increasing deflections. This is illustrated in Fig. 13. An approximate linear relationship between the area enclosed by the hysteresis loops with the increasing plasticity ratio has been proposed (4, 5). Therefore, on the basis of the experimental evidence, it appears that the reliability of the energy absorption capacity of properly designed and fabricated structural steel beams and their connection, is assured.

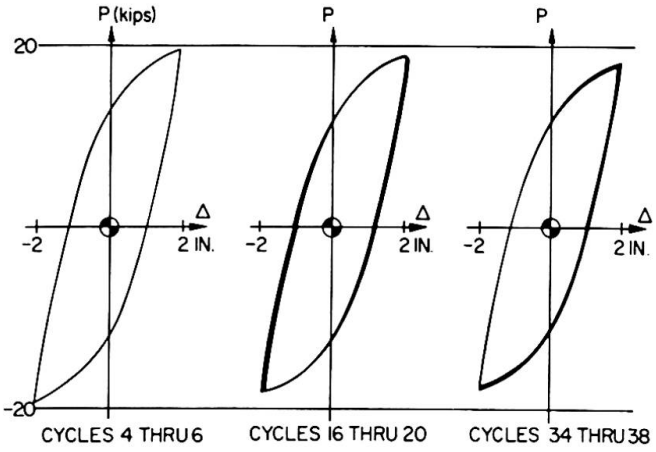

Fig. 12 Specimen F2-C4

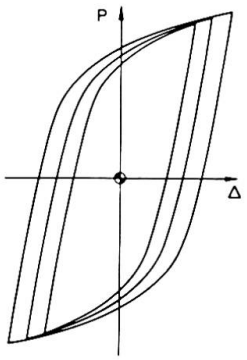

Fig. 13

Application of Experimental Results

Once one is satisfied that the hysteresis loops are reproducible during consecutive identical cycles of load application, and that the increase of the loops with increasing deflections is reasonably well established, this information can be put in mathematical form suitable for the analysis of structures. The well-known Ramberg-Osgood representation of non-linear load-displacement relationships together with Masing's hypothesis provide suitable mathematical formulations (5, 9).

Precisely this type of idealization has been applied by Berg (10) to some of the hysteresis loops generated in these experiments. By using such a formulation he studied the response of the assumed structure to a very severe ground motion are shown in Fig. 14(a), (b) and (c). The same results superposed on the same graph are shown in Fig. 15. The lateral displacements for the assumed structure having one degree of freedom are shown in Fig. 16 for a longer period of time. From this figure it is seen that often the displacements are not as severe as shown in Fig. 15 and are essentially elastic in their character.

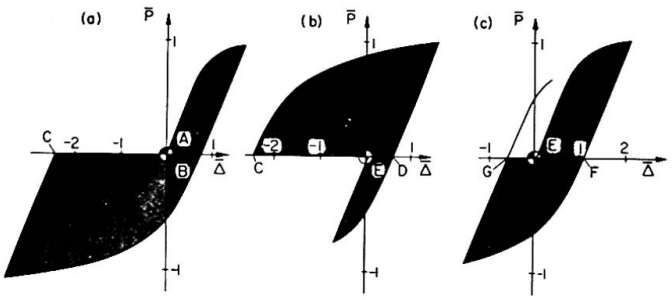

Fig. 14

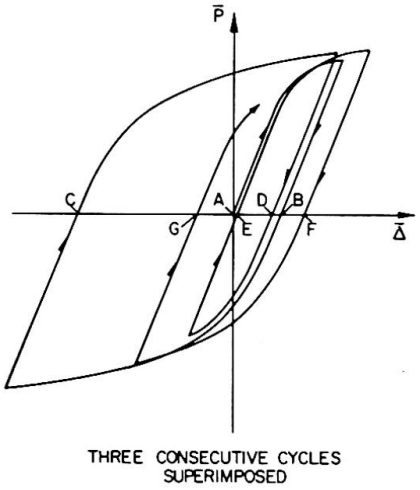

Fig. 15

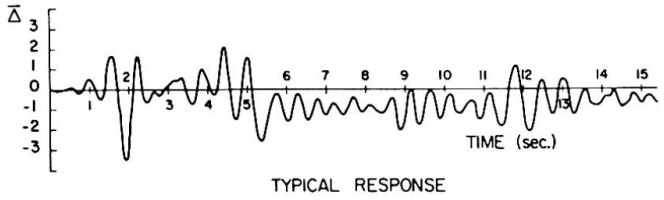

Fig. 16

Studies such as made by Berg for the above simple problem are the kind that are needed for real structures. From such studies the behavior of any one connection can be determined for an assumed earthquake. The amount of energy to be dissipated (shaded areas in Fig. 14) could be found and an assessment of the adequacy of the joint be made. Such a procedure would place the aseismic design of buildings on a more rational basis.

Acknowledgements

The work reported in this discussion was sponsored by the American Iron and Steel Institute. Among the number of people who have participated in this program, the writer is particularly indebted to R. B. Pinkney, a graduate student at the University of California, who participated in all phases of this investigation.

References

1. Bertero, V. V., and Popov, E. P., "Effect of Large Alternating Strains on Steel Beams", J. of Struct. Division ASCE, Vol. 91, ST1, Feb. 1965, pp. 1-12.

2. Popov, E. P., and Franklin, H. A., "Steel Beam-to-Column Connections Subjected to Cyclically Reversed Loading", Proceedings 34th Annual Convention, Struct. Eng. Assoc. of California, October 1965, pp. 79-86.

3. Popov, E. P., "Low-Cycle Fatigue of Steel Beam-to-Column Connections", Internat. Symposium on The Effects of Repeated Loading of Materials and Structural Elements, Mexico City, 1966, Vol VI.

4. Popov, E. P., and Pinkney, R. B., "Behavior of Steel Building Connections Subjected to Repeated Inelastic Strain Reversal-Experimental Data", University of California, Berkeley, SESM 67-31, December 1967.

5. Popov, E. P., and Pinkney, R. B., "Alternating Inelastic Strains in Steel Connections", J. of Struct. Division ASCE, (in preparation).

6. Popov, E. P., "Reliability of Steel Beam-to-Column Connections under Cyclic Loading", Fourth World Conference on Earthquake Engineering, Santiago, Chile, January 1969, (in preparation).

7. Courtesy of Professor Joseph Penzien.

8. Current AISI Project 145 under the supervision of V. V. Bertero and E. P. Popov.

9. Jennings, P. C., "Periodic Response of a General Yielding Structures", J. of Eng. Mech. Division ASCE, Vol. 90, EM2, April 1964, pp. 131-166.

10. Berg, G., "A Study of the Earthquake Response of Inelastic Systems", Preliminary Reports - Steel Research for Construction, February 1966, AISI.

SUMMARY

In this discussion attention is called to the availability of some of the new experimental results on the inelastic behavior of steel cantilever beams and their connections to column stubs during repeated and reversed cyclic loading. The described experiments attempt to simulate the conditions which develop in structural steel frames during an earthquake.

RÉSUMÉ

Cette contribution signale l'existence de nouveaux résultats expérimentaux concernant le comportement inélastique de poutres consoles en acier et leur liaison à des colonnes courtes soumises à des charges périodiques répétées et alternées. Le but des expériences décrites est de simuler les conditions qui se développent dans des ossatures en acier pendant un tremblement de terre.

ZUSAMMENFASSUNG

In diesem Beitrag soll auf einige der neueren experimentellen Ergebnisse über das inelastische Verhalten von Kragträgern aus Stahl aufmerksam gemacht werden, sowie ihren Anschlüssen an Stützenabschnitte, wenn die Träger wiederholten, zyklischen Wechselbelastungen ausgesetzt sind. Anhand der angeführten Versuche wird versucht, die Bedingungen nachzuahmen, die während eines Erdbebens in Rahmenkonstruktionen aus Stahl auftreten.

Leere Seite
Blank page
Page vide

Inelastic Behavior of the Steel Framed Structure Subjected to the Seismic Force

Comportement inélastique de structures en câdres d'acier soumises à des forces sismiques

Unelastisches Verhalten des Stahlrahmentragwerkes unter Erdbebenkraft

BEN KATO
Associate Professor

HIROSHI AKIYAMA
Research Associate

The University of Tokyo
Japan

Introduction

To clear the safety of the structure against earthquake, it is necessary to know the inelastic behavior of beams, columns and entire frames until their collapse state under alternating loading as the author states. This discussion concerns to evaluation of the inelastic behavior of steel structural members.

It is known that the conventional simple plastic theory cannot predict the actual inelastic behavior of the steel structures even in monotonous loading, and it can be said that this mainly comes from the fact that the strain hardening property of the material is not taken into account in that analysis, and the effect of the applied axial load is not evaluated reasonably.

We suggest the solution for the beam-column subjected to axial compression and bending moment which makes allowance for the strain hardening and the effect of the axial compression. The load deflection diagram under alternating loading is shown to be obtained from the load deflection diagram under monotonous loading by the simple definite procedure.

Furthermore, the response analysis of the one mass vibration model of the steel structure is done using the clarified inelastic characteristics, and the difference of the response is shown to be attributed to the difference of evaluation of the effect of the strain hardening upon the structure.

Inelastic Behavior of Steel Members

Monoaxial bending only is treated here, and the effect of shear stress is ignored. Lateral buckling is also out of the matter. Breaking-off and local buckling of the section element of the member are considered to be the most effective origins of the collapse of the member and these origins can be predicted by some material tests.

General feature of the stress strain relation of steel may be expressed by the diagram as shown in Fig.(1).

As the bending deformation is obtained by integration of the

curvature along member axis, to determine the moment curvature relation is the essential procedure.

Moment Curvature Relation--- Case I when the bending moment is applied in monotonous way: The bending moment is to be applied about x-x axis in Fig.(2), and the section of the member is assumed to be symmetric about the axis perpendicular to the bending axis. Axial compression is kept in constant, and the moment increases gradually.

Let the solid line of Fig.(3) be the strain distribution at the arbitrary inelastic state under moment M, and the broken line be that of after infinitecimal increase of the curvature due to the increase of moment. Then the following relation are derived from the equilibrium condition of stress.

$$dH_1=-\frac{d\phi}{\phi}H_1\ ,\quad dH_1'=-\frac{d\phi}{\phi}H_1'\ ,\quad dH_2=-\frac{d\phi}{\phi}H_2\ ,\quad dH_2'=-\frac{d\phi}{\phi}H_2'$$

$$dS_e=(dH_1B_1+dH_2B_2)e_1+(dH_1'B_1'+dH_2'B_2')e_2$$

$$dI_e=(dH_1B_1H_1^2+dH_2B_2H_2^2)e_1+(dH_1'B_1'H_1'^2+dH_2'B_2'H_2'^2)e_2$$

$$dO=\left\{-(dH_1B_1H_1-dH_2B_2H_2)e_1-(dH_1'B_1'H_1'-dH_2'B_2'H_2')e_2\right\}/S_e$$

where ϕ: curvature $d\phi$: increment of ϕ

ε_y: strain at yield point

ε_{st}: strain at strain hardening point

e_1: $(E_1-E_2)/E_1$ e_2: $(E_2-E_3)/E_1$

H_1: distance from the transient neutral axis to the compression fibre where the strain is equal to ε_y.

H_2: distance from the transient neutral axis to the tension fibre where the strain is equal to-ε_y.

H_1': distance from the transient neutral axis to the compression fibre where the strain is equal to ε_{st}.

H_2': distance from the transient neutral axis to the tension fibre where the strain is equal to-ε_{st}.

S_e: effective area, which means the sectional area of the ficticious elastic bar which has the equivalent axial rigidity to the actual bar in the specified inelastic state.

I_e: effective moment of inertia, which means the moment of inertia of the ficticious elastic bar which has the equivalent flexural rigidity to the actual bar in the specified inelastic state.

dO: movement of the transient neutral axis

B_i, B_i' : width of the section at H_i, H_i' respectively.

After the increase of the curvature $d\phi$, these quantities will change as follows.

$$H_1\rightarrow H_1+dH_1+dO\ ,\quad H_2\rightarrow H_2+dH_2-dO$$

$$H_1'\rightarrow H_1'+dH_1'+dO\ ,\quad H_2'\rightarrow H_2'+dH_2'-dO$$

$$S_e\rightarrow S_e+dS_e\ ,\quad I_e\rightarrow I_e+dI_e\ ,\quad \phi\rightarrow\phi+d\phi\ ,\quad M\rightarrow M+E_1I_e\,d\phi$$

M-ϕ relation may be pursued successively using the above relaion throughout the whole strain range. Numerical calculation is performed easily by the aid of the electronic digital computer.

Case II when the bending moment is applied alternatingly: It is very complicated to describe the exact M-ϕ relation under alternating bending. So by the aid of the simplified model given below, an outline of the relation is sought after.

1. Member section is sandwitch type as shown in Fig(4).
2. Stress strain relation of steel under alternating loading is as shown in Fig.(5b). To be more precise, with regard to the stress in definite sign the stress strain relation has the same configuration as that under monotonous loading as shown in Fig.(5a).

On such a model it is easily understood that the M-ϕ relation under alternating loading is obtained as shown in Fig.(6b). Fig.(6a) shows the M-ϕ relation under monotonous bending. Comparing Fig.(6a) and Fig.(6b), it can be seen that in Fig.(6b) with regard to the bending moment in one direction the M-ϕ relation has the same configuration as that shown in Fig.(6a).

The actual shape of section differs from that provided by the condition 1. Hence when the bending moment is removed, the residual stress is introduced over the section. In this paper, however, the effect of such a residual stress is assumed to be negligible, so the M-ϕ relation obtained above becomes applicable to any section.

Load Deflection Curve of Steel Members--- Deflection of the member is readily obtained by integration of the curvature corresponding to the bending moment produced by the external loads. For the exact solution numerical integration technique is effective, but in some cases approximate solution provides facility for engineering purposes. Especially the solution under alternating loading is uselessly troublesome. Hence for this case some devices in approximation are needed.

When the bending stress is determined uniquely by the external loads, the correlation between the load deflection curve under alternating loading and that under monotonous loading is similar to the correlation as exists in M-ϕ relation. As is shown in Fig.(7), the load deflection diagram under alternating loading is readily obtained from that under monotonous loading. With regard to a definite direction of loading, the load deflection curve in Fig.(7b) has the same configuration as that in Fig.(7a).

But in general, geometry change of the member affects upon the bending moment distribution. In Fig.(8) two cantilever columns are shown for example. When the end load is applied alternatingly under constant axial load P, lateral deflection produces secondary bending. When the end load is removed after some extent of the inelastic deformation in one direction, deflection remains and to remove the residual moment at the fixed end, end loads of $-P\delta/\ell$ in the case of Fig.(8a) and $-P\delta$ in the case of Fig.(8b) are required respectively. In such a state residual stress still remains along the member axis as shown in Fig.(9). Here, we assume that the residual stress shown in Fig.(9) has no effect upon the load deflection relation under further application of the end load in the opposite direction. Based on the assumption, we can depict the load deflection curve as shown in Fig.(10), that is, the load deflection curve under alternating loading is obtained from that under monotonous loading in the same manner as is shown in Fig.(7). In Fig.(7) the abscissa is the basal line whereas in Fig.(10) the broken line which shows the tentative unloaded state of the member is the basal line, and with regard to the load deflection relation in one side of this line, the curve under alternating loading has the same configuration as that under monotonous loading. From this figure it can be seen that the summation of the plastic deformation in one direction until collapse does not exceed the plastic deformation capacity under monotonous loading.

Comparison with Test Result--- Load deflection curves were obtained using the test specimens as shown in Fig.(11). In specimen(A) the column is subjected to axial thrust and the transverse shear force increasing proportionally according to

the following condition.

$$P=V\cos\psi \ , \quad Q=V\sin\psi$$

Where V is the applied load.

In specimen(B) the column is subjected to constant axial load and alternating end moment conducted through beams.

Stress strain relation of the material was obtained from the stub column test, and is shown in Fig.(12). The maximum stress was reached by occurence of the local buckling of flanges.

M-ϕ relation obtained from the procedure mentioned above is shown in Fig.(13). Load deflection curve of the specimen(A) is shown in Fig.(14), and the curve of the specimen(B) is shown in Fig.(15) in which the theoretical curve under monotonous bending is shown by the curve ABC.

Collapse of the member was assumed to occur when the stress at the point where the maximum moment grows reachs σ_B over entire section. M_B corresponds to such a stress distribution. In Fig. (14) and (15) theoretical curves after collapse are drawn on the assumption that the maximum moment of the specimen is kept to be M_B.

In these figures the test results agree with the theoretical prediction fairly well, and the effect of the strain hardening upon the inelastic behavior is very remarkable.

Response Analysis of the Framed Structure

Restoring Force Characteristics--- The cantilever column shown in Fig.(16) represents the fundamental element of the framed structure subjected to seismic force. To see the general feature of resistance of the framed structure to seismic force, a simple outline of the inelastic behavior of the cantilever column is sought after through the approximate approach.

The M-ϕ relation under the constant thrust obtained above may be approximated by two linear segments ignoring the elastic part of it. The first segment is parallel to the abscissa at M_{PC}.

At first the deflection of the member is evaluated ignoring the effect of the secondary bending caused by the geometry change. In Fig.(17) the part of the column ab is in inelastic range under the given loads P and Q, the the distribution of the curvature along the member is expressed as shown in Fig.(17b). This is reduced to the simplified model as shown in Fig.(17c) in which the curvature of the inelastic part ab is approximated by the mean value of the curvatures at the both ends of ab, then the mean value ϕ_o may be written as follows.

$$\phi_o = \frac{\phi_{st}+\phi_f}{2} = \frac{M_f - M_{PC}}{2D_{st}} + \phi_{st} \qquad (1)$$

Where ϕ_{st}: the curvature at the starting point of the strain hardening.

D_{st}: the flexural rigidity in strain hardening range. Namely the slope of the second segment.

M_{PC}: the fully plastic moment under axial force.

M_f: the fixed end moment

The lateral deflection δ_b and the slope θ_b at point b are given as follow.

$$\delta_b = (\phi_o l_1^2)/2 \ , \quad \theta_b = \phi_o l_1$$

Then the lateral deflection at the top of the member may be given as follows.

$$\delta = \phi_o l_1 l_2 + (\phi_o l_1^2)/2 \qquad (2)$$

Where l_1: the length of the inelastic part of the member.

l_2: the length of the elastic part of the member.

As the bending effect of the thrust P is ignored, the follwing

relation will hold for any shear force Q'.

$Q'l_2 = M_{pc}$, $Q'l = Q'(l_1 + l_2) = M_f$

These are translated as:

$l_1/l = (\alpha-1)/\alpha$, $l_2/l = 1/\alpha$, $\alpha = M_f/M_{pc}$

From equation(1) and (2), introducing the expression $M_{pc} = D\phi_y$, and $\beta = \phi_{st}/\phi_y$, the lateral deflection is written as follows.

$$\delta = \left(\frac{\alpha-1}{2} \times \frac{D}{D_{st}} + \beta\right)\left(\frac{\alpha^2-1}{2\alpha^2}\right) l^2 \phi_y \qquad (3)$$

Where D: flexural rigidity in the elastic range

As the second step, the effect of the secondary bending must be taken into account. This effect is illustrated in Fig. (18) where the curve ac shows the deflected configuration of the member. Horne*had approximated this configuration by the straight line connecting the both ends of the members as shown in Fig. (18a). Then the equivalent lateral force Q which provide the same bending moment at the fixed end is given as follows.

$$Q = (M_f - P\delta)/l = (\alpha M_{pc} - P\delta)/l \qquad (4)$$

Equation (3)and (4) give the Q-δ relation.

This approximation, however, underestimates the secondary bending and the another approximation as shown in Fig.(18b) is proposed, where the point* shows the coordinate $(\delta, (\alpha-1)l/2\alpha)$. $(\alpha-1)l/2\alpha$ denotes the midheight of the inelastic portion, and the deflected shape of the member is approximated by the straight line also. This choice seems to be rather arbitrary, but it will be shown later that this gives the better approximation to the exact solution. In this approximation the equivalent horizontal shear force is given as follows.

$$Q = \left\{\alpha M_{pc} - \left(\frac{2\alpha}{\alpha+1}\right)P\delta\right\} / l \qquad (5)$$

Comparison with the exact solution is made in Fig.(19) with regard to the Q-δ relation using the same section member as shown in Fig.(11), and the same stress strain relation as shown in Fig.(12).

In the case of no axial thrust these two methods coincide, however when the axial force becomes larger, it can be seen that the later method gives better approximation than the former one. In Fig.(20) Q-δ diagram for the same member derived from the conventional theory ignoring the strain hardening is given. Comparing these two figures, it can be seen that the effect of the strain hardening is very significant.

Besides, from Fig.(19) it can be seen that the inelastic deflection curve may be approximated by the linear relation without substantial error. Hence the fundamental feature of the restoring force characteristics of the framed structure may be suggested to be the relation as shown in Fig.(10).

Response Analysis of the 1 Mass System--- Using the restorig force characteristics given in Fig.(21) the response analysis was done . For an example, one mass viburation system as shown in Fig.(21) is chosen.

The ground motion is of N-S component of El Centro 1940, May(the peak value of acceleration is 330 gals)

Governing equation of the sytem is as follows.

$$m(\ddot{y}+\ddot{y}_o)+f(y)=0$$

Where y: deflection , y_o: ground motion

f(y): restoring force characteristics

Result of the analysis is given in Fig.(22). Fig.(22a) shows the residual plastic deflection after the ground motion is faded away. Fig.(22b) shows the maximum deflection during the

earthquake and Fig.(22c) shows the summation of the plastic deflection in one direction.

The ordinate of these diagram expresses the yield force coefficient which is given as follows.

$f=F_y/mg$

Where g: acceleration of gravity

The abscissa expresses the plastic deflection divided by the initial elastic limit deflection which corresponds to the initial elastic limit stress F_y.

In these figures, the parameter K denotes the strain hardening effect. When the strain hardening does not exist, the value is equal to the slope of the basal line ff' in Fig.(21) which denotes the effect of the secondary bending by the weight of the mass.

From these figure it can be seen that the plastic deflection is considerably affected by the strain hardening effect and especially development of the residual deflection is moderated by the strain hardening.

Conclusion

The more precise aspect of the inelastic behavior of the steel members has been pursued by the experiment and the analysis which makes allowance for the strain hardening property of steel.

The effect of the strain hardening property upon the deflection response of the steel framed structure to an earthquake was evaluated, and that was shown to be very remarkable.

Reference

* Horne M.R. , Medland I.C. : Collapse Loads of Steel Frameworkes Allowing for the Effect of Strain Hardening.
Proc. Institution of Civil Engineers 1966, May

Fig.(1) Stress Strain Relation

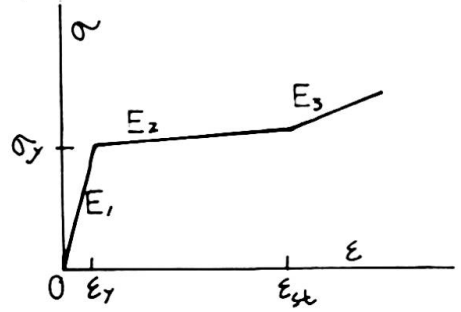

Fig.(2) Section Shape

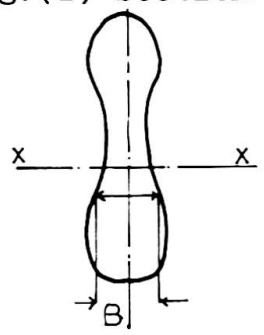

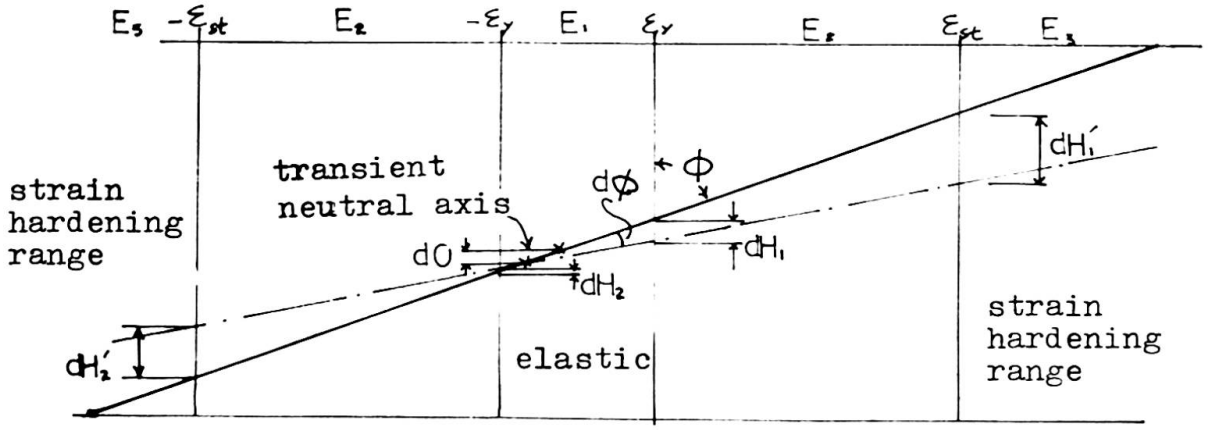

Fig.(3) Strain Distribution over the Section

Fig.(4) Simplified Section

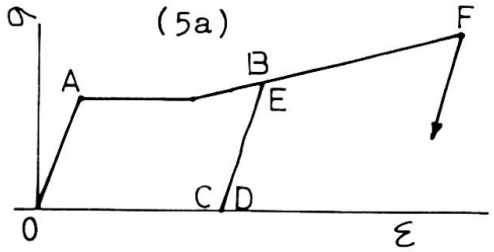

Fig.(5) Stress Strain Relation

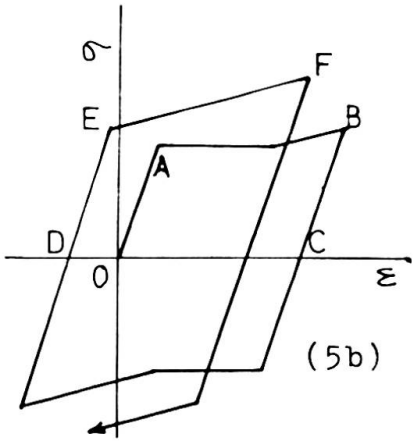

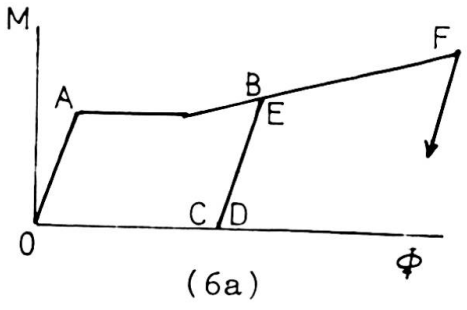

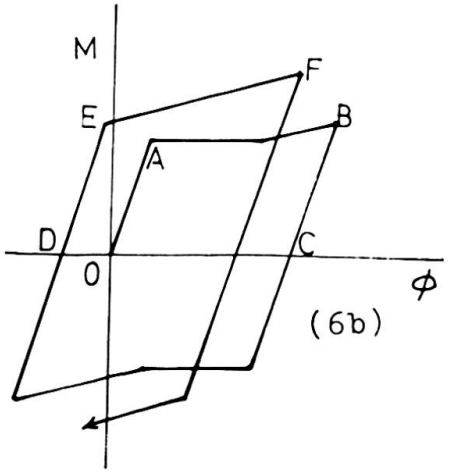

Fig.(6) M-φRelation

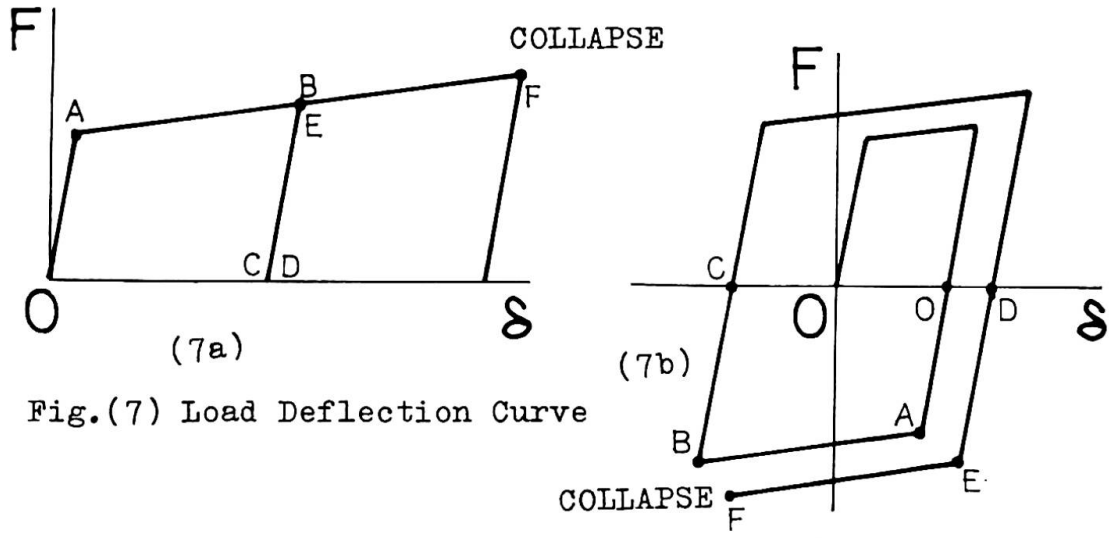

Fig.(7) Load Deflection Curve

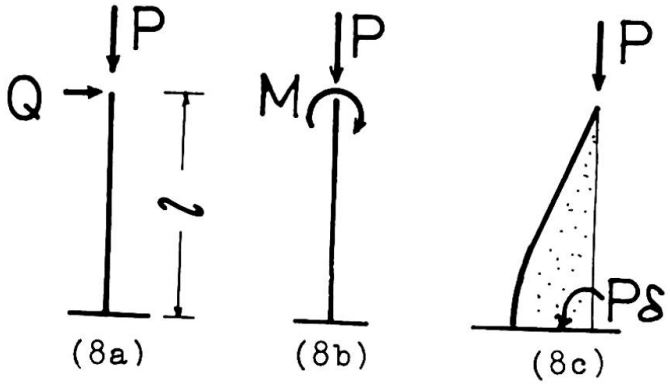

Fig.(8) Cantilever Column

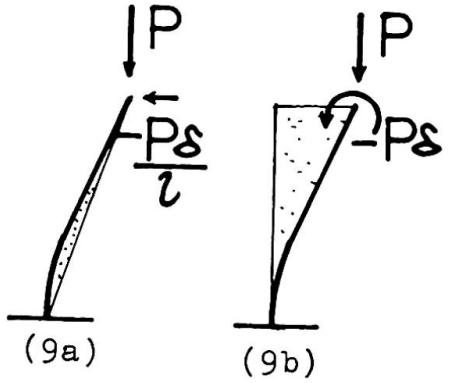

Fig.(9) Residual Stress

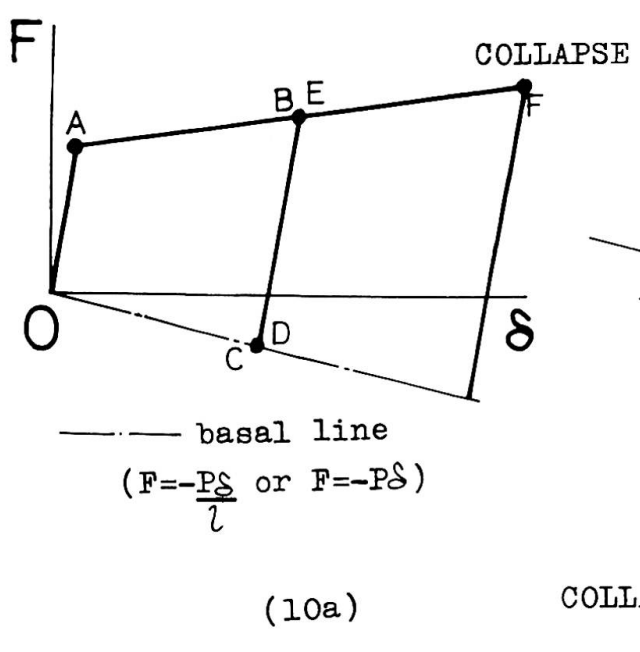

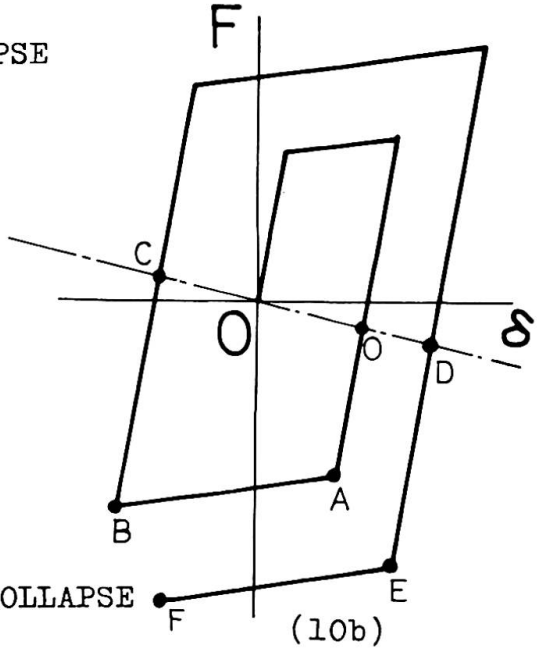

Fig.(10) Load Deflection Curve under Alternating Loading

Fig.(11) Tect Specimens

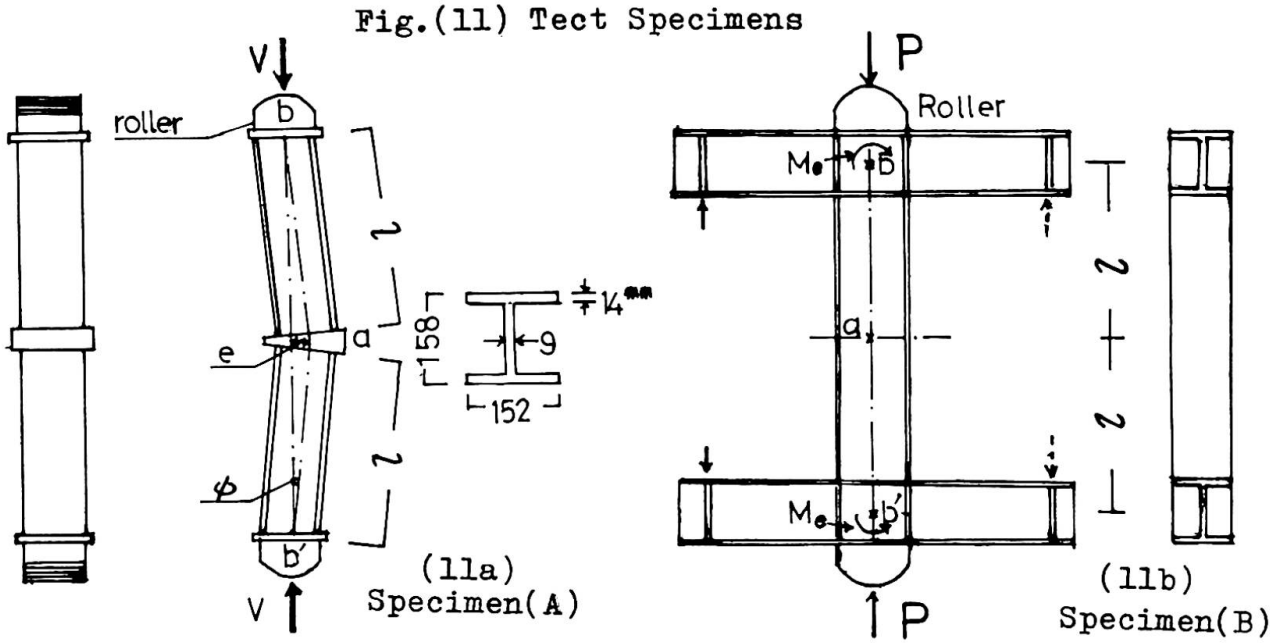

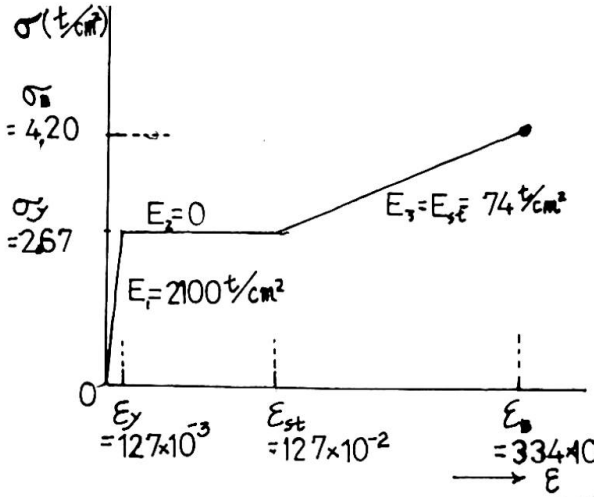

Fig.(12) Stress Strain Relation

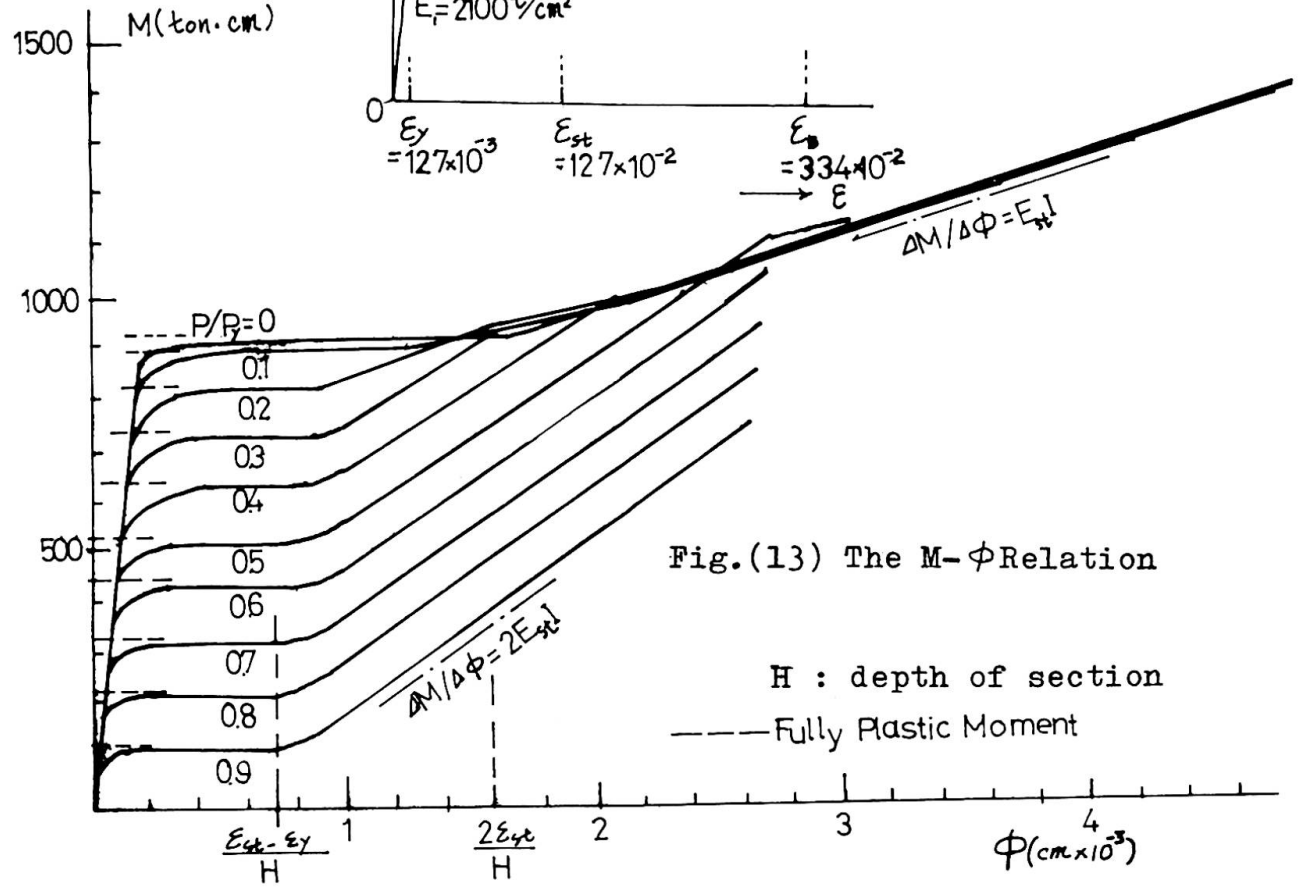

Fig.(13) The M-φ Relation

H : depth of section

———Fully Plastic Moment

Fig.(14) Load Deflection Curve of (A)

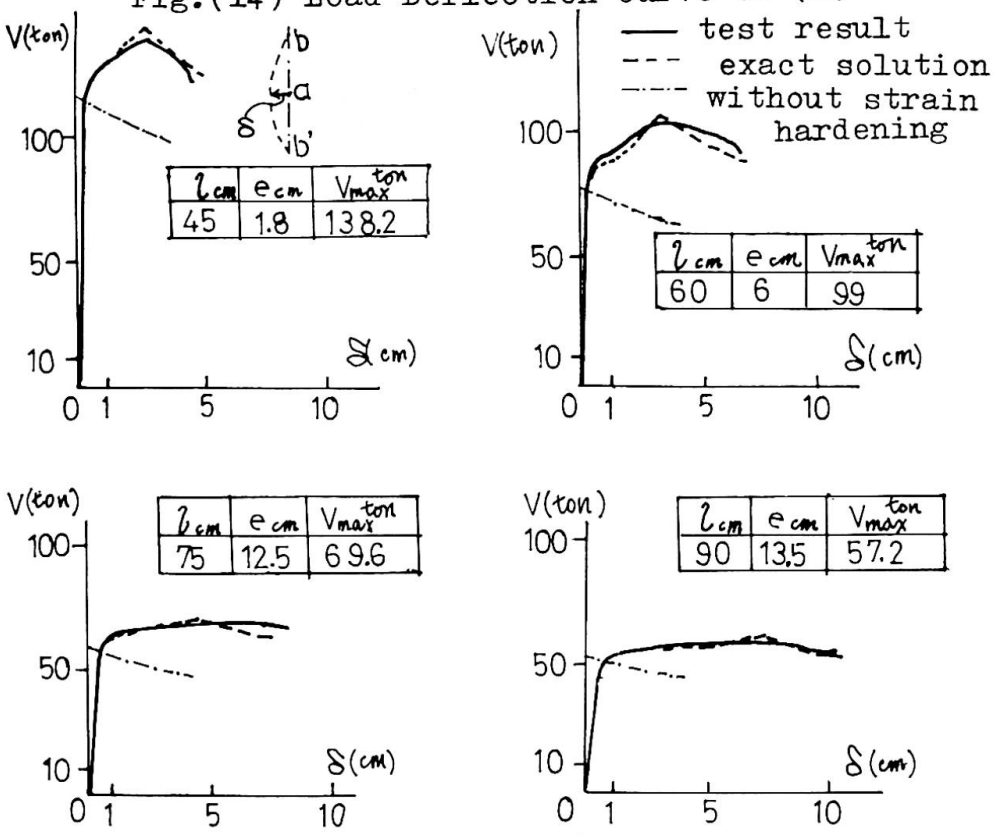

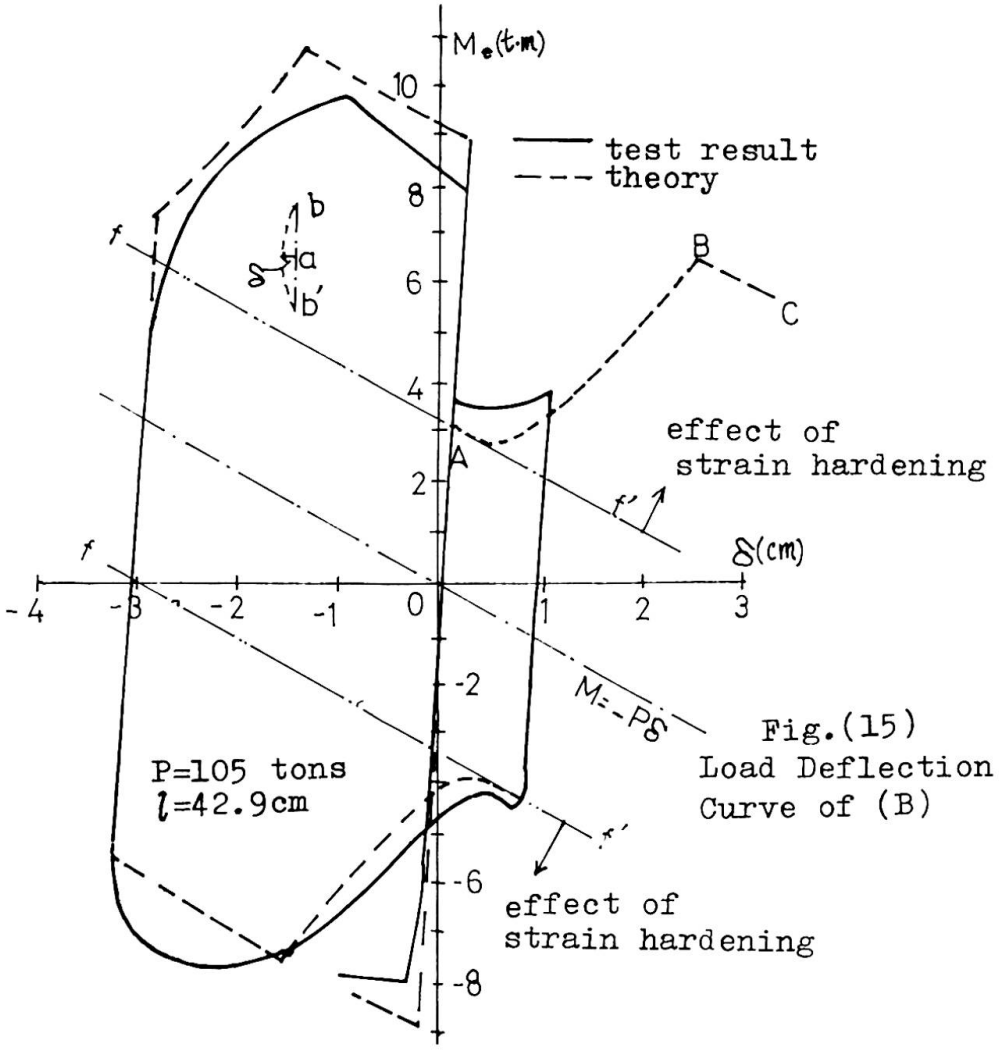

Fig.(15) Load Deflection Curve of (B)

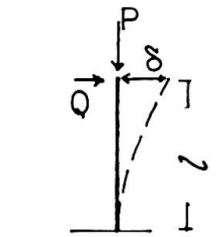

Fig.(16)

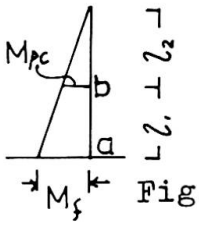

Fig.(17a)

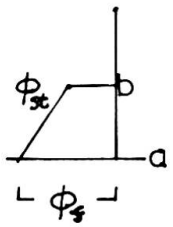

Fig.(17b)

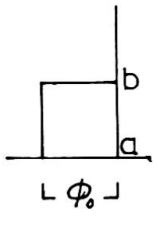

Fig.(17c)

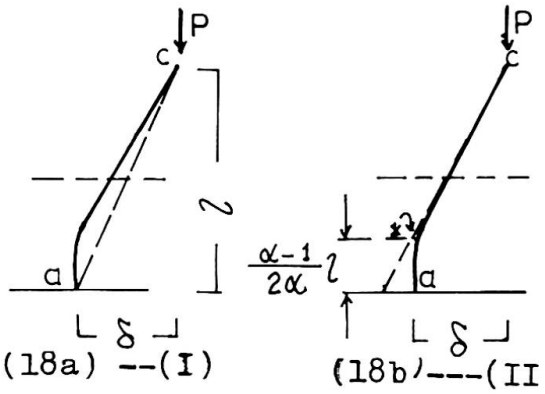

Fig.(18) Approximated Deflection

Fig.(19) Load Deflection Curve

——— Exact Solution • Collapse State

– – – Approximation I —·—·— Approximation II

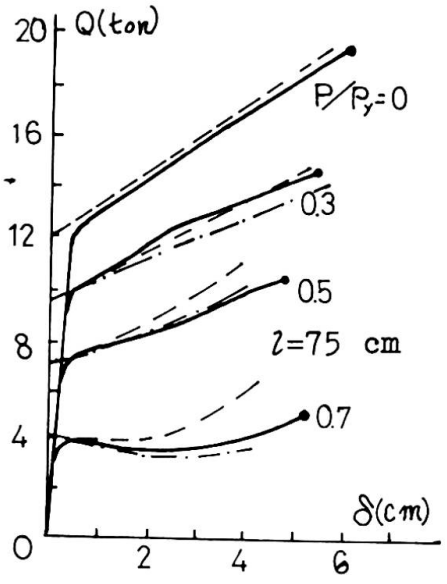

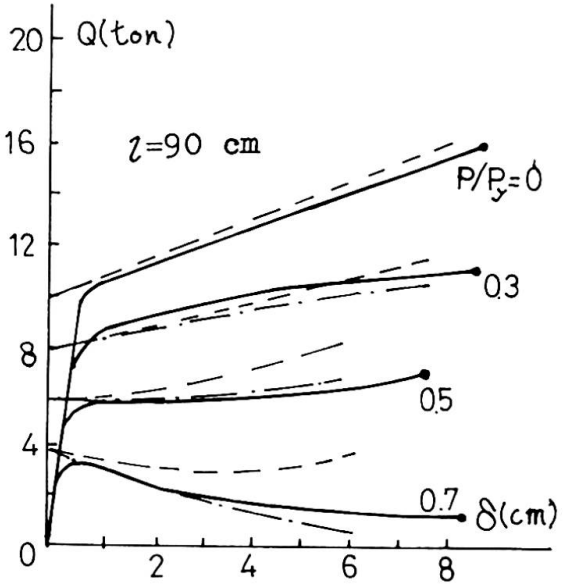

Fig.(20) Load Deflection Curve P_y: yield axial force

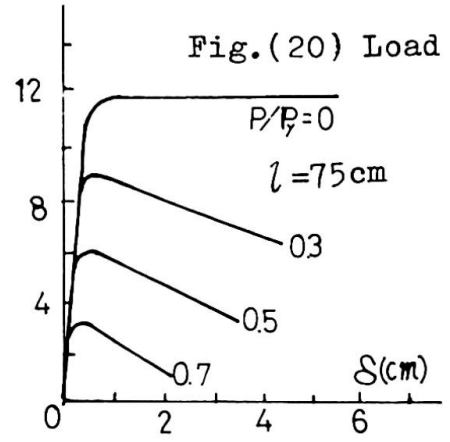

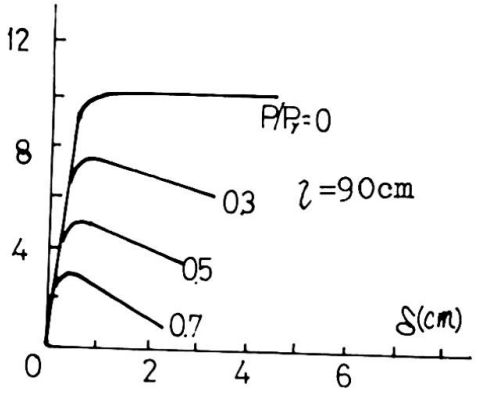

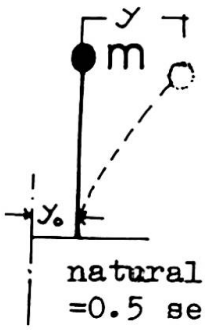

natural period
=0.5 sec.

(21a) One Mass System

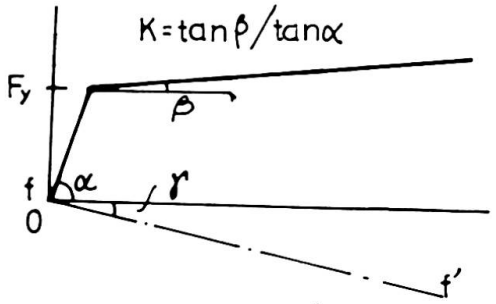

$\tan\gamma/\tan\alpha = -0.05$

Restoring Force
Characteristics

(21b)

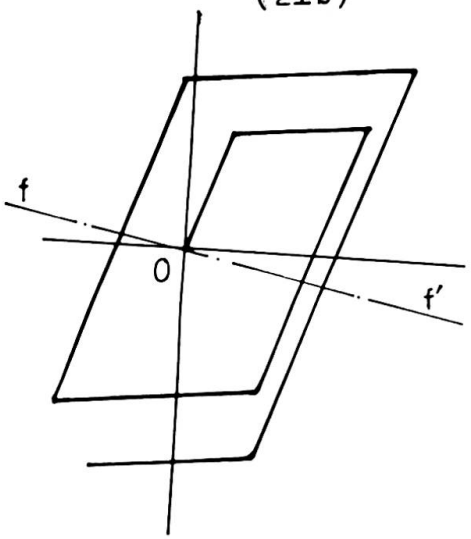

Fig.(21)

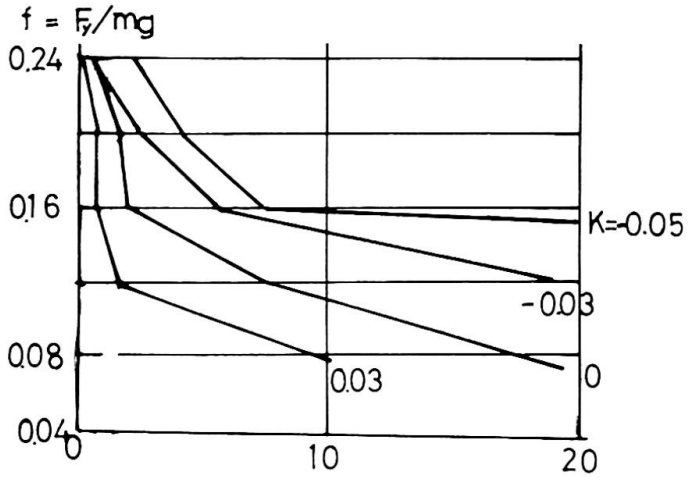

(22a)

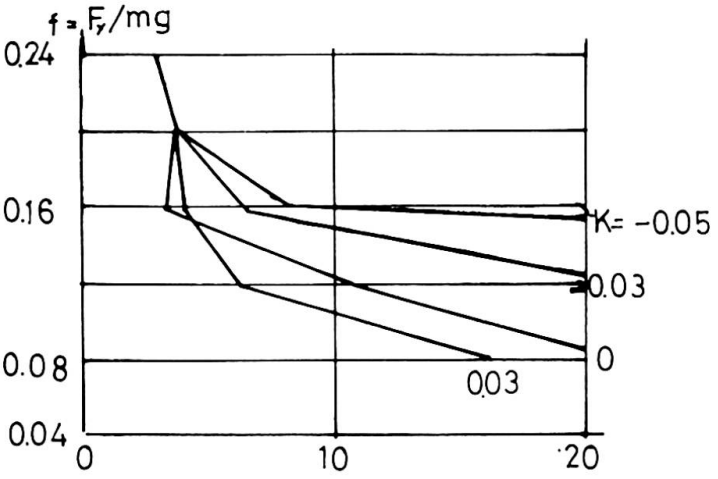

(22b)

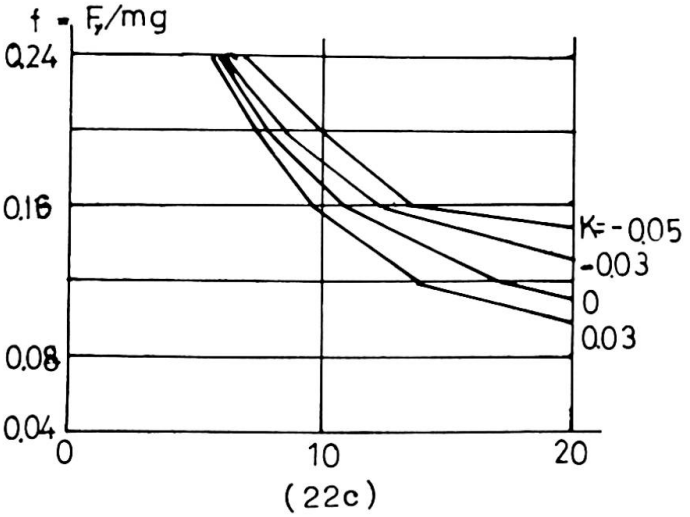

(22c)

Fig.(22) Deflection Response

SUMMARY

The more precise aspect of the inelastic behaviour of the steel member has been pursued by the analytical method which makes allowance for the strain hardening property of steel.

And the effect of the strain hardening property upon the deflection response of the steel framed structure to an earthquake was evaluated.

RÉSUMÉ

Des connaissances plus précises du comportement plastique de membres en acier ont été obtenues par la méthode analytique, ce qui permet de tenir compte du durcissement de l'acier. Cet effet du durcissement sur la déformation du portique d'acier due à un tremblement de terre a été évalué.

ZUSAMMENFASSUNG

Genaue Kenntnisse des plastischen Verhaltens von Stahlbauteilen wurden mit analytischen Berechnungen angestrebt, wodurch die Verhärtung des Stahls berücksichtigt werden konnte. Die Wirkung der Verhärtung auf die Verformung des Stahlrahmens wurde abgeschätzt.

Leere Seite
Blank page
Page vide

The Design of Multi-Story Buildings against Wind

Dimensionnement de bâtiments élancés par rapport aux efforts du vent

Bemessung von Hochhäusern auf Wind

A.G. DAVENPORT
Professor
Director, Boundary Layer Wind Tunnel Laboratory
the University of Western Ontario
Faculty of Engineering Science
London, Ontario, Canada

Submitted as a discussion of the paper "Dynamic Effects of Wind and Earthquake", by D. Sfintesco.

The author's paper reminds us of the similarities and differences in the approach to the wind and earthquake design of tall buildings. Taken together with the papers by Ferry Borges and also by Newmark and Hall, a fairly comprehensive survey of the subject is presented.

The historical allusion made by Sfintesco to the notable work by Gustav Eiffel and Sir Benjamin Baker reminds us of their insight into the action of the wind on structures. Their recognition of the influence of the size of the structure on the response and its dynamic response to wind, in many senses is clearer than several contemporary viewpoints.

In this discussion, the writer draws attention to two approaches to designing tall buildings against wind which perhaps answer some of these questions posed by Eiffel and Baker regarding both the size effect and the resonant response. These approaches are:

a) a Gust Factor approach; and
b) the use of wind tunnel modelling.

A design approach embodying gust factors has been described in several papers. It is already in use in the Danish Standards and is currently under consideration for incorporation in the National Building Code of Canada.

DESIGN CRITERIA FOR WIND LOADING

Sfintesco refers to most of the significant wind effects on tall buildings; namely, collapse, damage to masonry and finishes, damage to windows and cladding, fatigue damage, and comfort of occupants.

Some tentative design criteria for these effects are as follows:

1) Collapse: Current design conceives of the structure withstanding a wind having a recurrence interval of about 30 years, with a safety factor on the minimum stress of roughly 2.0. In fact, this may be the least critical requirement in most tall buildings. It might be more logical to use a far more improbable wind speed and a lower safety factor; for example, a once-in-500-year wind speed and a safety factor of 1.1 might give a more rational evaluation of risk.

2) Damage to masonry and finishes: Masonry and plaster appears to become sensitive to cracking under racking loads when the story deflection is in the range 1/8" - 1/2". This corresponds to an average building drift limitation of the order of 1/250 to 1/1000. If the average interval for redecorating is 3 years and if a 10% risk that damage would be done within this period was acceptable, an average recurrence interval of 30 years would be appropriate. The actual deflection criterion should properly be related to the kind of partition and masonry or other elements used.

3) Windows and cladding: Cladding and window lights today represent a very large proportion of the total cost of tall buildings. An acceptable breakage rate of 1 light per building every ten years might be acceptable: unacceptable deflections on the windows should probably not be permitted to occur more often than once every 5 years.

4) Fatigue: This is the most common cause of failure of structures damaged by wind. It can probably best be evaluated by use of cumulative damage laws. Procedures for its evaluation have been described by Davenport. It is likely to arise whenever dynamic stress amplitudes are high. These circumstances indicate the desirability of wind tunnel tests.

5) Comfort of occupants: It appears that the threshold of perception

of human beings to horizontal vibration occurs when the maximum acceleration is roughly in the range 0.5 - 1.5% of gravity: 1.5 - 5.0% of gravity may be annoying.

Of course, all of the above must be regarded as opinions rather than inflexible yardsticks: the subject matter concerned is essentially statistical, and the decision making cannot be made without some uncertainty. The suggested criteria are summarized in Table 1.

TABLE 1

TYPICAL CRITERIA FOR DESIGN OF TALL BUILDINGS AGAINST WIND

Unserviceability Symptom	Acceptance Criteria	Recurrence Interval: Years
1) Collapse	Safety factor = 1.1	500
2) Cracking of masonry & finishes	Max. def'n. $< \frac{1}{250} \rightarrow \frac{1}{1000}$ of height	30
3) Windows and cladding:		
a) perceptible deflections;	a) dependent on size of light, colour and type of glass	a) 5
b) breakage	b) <1 breakage per building	b) 10
4) Fatigue	Cumulative damage <100%	500
5) Comfort of occupants	Max. acc'n. <.5 → 1.5%g	10

DESIGN APPROACH #1 -- GUST LOADING FACTOR

This approach consists of the following phases:

1) The prediction of extreme average wind speeds from long term meteorological records such as those indicated in Fig. 1.

2) The adjustment of these wind speeds obtained at the meteorological observation station to the terrain conditions and height of the structure by means of profiles such as those shown in Fig. 2.

3) The determination of mean pressures using pressure coefficients appropriate to the particular flow conditions and structural shape as illustrated in Fig. 3.

4) The determination of the gust amplification factor using the gust pressure factor G defined below and in Fig. 4.

The gust pressure factor is intended to take account of the superimposed dynamic effect of gusts. It is used in conjunction with the mean load so that the total wind loading at any point on the building is,

$$p(Z)_{max} = G\,\bar{p}(Z)$$

where $\bar{p}(Z)$ refers to the mean pressure at height Z and given by such pressure coefficients as those in Fig. 3.

The factor G is the gust factor given by,

$$G = 1 + gr\sqrt{B+R}$$

in which g = peak factor, r = roughness factor, B = excitation by background turbulence, and R = excitation by turbulence resonant with structure.

The quantity,

$$R = \frac{S\,F}{\beta}$$

in which F = gust energy ratio, s = size reduction factor, and β = damping factor.

An explanation of these factors follows. In all cases, the mean velocity $\bar{V}$ is the velocity at the roof level. Graphs of g, r, B, F and s are shown in Fig. 4.

1) The peak factor g is the ratio of the peak dynamic response to the RMS response of the structure. It is a function of the average fluctuation rate of the response and the averaging period of the mean T. T should be between 5 min. and 1 hour. An expression for ν is

$$\nu = n_o \sqrt{\frac{R}{B+R}}$$

where R and B are defined below. For a peaked response, the

value of $\frac{R}{R+B}$ is near to unity and $\nu \simeq n_o$, n_o being the natural frequency.

2) The expression $r\sqrt{B+R}$ is in fact the RMS response of the structure to gusts. r is a roughness factor dependent on the terrain. r^2B is the contribution to the variance (mean square) response due to "background excitation", while r^2R is the contribution to the variance from the resonant response of the structure at its natural frequency.

3) The significant effect of size of the structure in reducing the dynamic load is seen both in B and the size reduction factor s.

4) The gust energy ratio F reflects the distribution of energy with frequency in the wind and hence the energy available to excite resonance.

5) The critical damping ratio β should include contributions to the damping from both mechanical and aerodynamic origin. For tall buildings, however, neglect of the aerodynamic damping is generally not significant. Suggested values of the mechanical damping are as follows:

Concrete	$\beta = .010 - .020$
Steel	$\beta = .005 - .010$

If the deflected shape of the structure both in the fundamental mode of vibration and under the action of steady wind is approximately rectilinear, as usually is the case with tall prismoidal buildings, an approximate expression for the maximum deflection and acceleration amplitudes can be derived. To do so, it is necessary to define an effective stiffness K which is the base bending moment per radian of rectilinear rotation of the structure. Knowing the base bending moment M under either inertia loading (dynamic) or the static wind loading either deflections or acceleration amplitudes may be found. Expressed in radians, the amplitude will then be simply M_o/K.

It is convenient to express the base bending moment in terms of the aerodynamic coefficient C_M so that,

$$C_M = \frac{1}{bh^2} \int_A Z\, C_p\, dA$$

where dA is an element of the projected frontal area, C_p is the local pressure coefficient on the front or rear surfaces at position Z and the integral is taken over front and rear surfaces.

The maximum deflection as a fraction of height is then computed from the expression

$$\frac{deflection}{h} = G\, \tfrac{1}{2}\rho V_o^2\, C_M\, bh^2/K$$

The maximum acceleration amplitudes invariably occur at the natural frequency and an approximate expression for the peak acceleration in the wind direction is,

$$maximum\ sway\ acceleration = 4\pi^2 n_o^2\, gr\sqrt{R}\, C_M\, \tfrac{1}{2}\rho V_o^2\, bh^3/K$$

$$= gr\sqrt{R}\, C_M\, \tfrac{1}{2}\rho V_o^2\, bh^3/I_o$$

where I_o is the moment of inertia of the building about the base, ie. $I_o = \sum m(Z)\, Z^2$, where $m(Z)$ is the mass in dynamic units at height Z.

Experience in the use of this approach generally indicates the following results:

1) Loading is on average in accordance with standard loadings used but the differentiation in loading between structures and between urban and rural terrains in significantly broader than standard approaches imply.

2) Tall slender structures with light damping incur relatively large dynamic gust factors (up to 3 times the mean load). Broad faced structures of relatively stiff construction incur relatively little dynamic amplification, perhaps only 30% greater than the mean load.

3) Structures in urban areas are affected more by turbulence than in rural area, but the mean loading is substantially lower.

4) Use of the correct velocity profile, wind tunnel testing conditions and dynamic gust factor are all highly significant and serious discrepancies can arise if this is not done.

DESIGN METHOD #2 -- BOUNDARY LAYER WIND TUNNEL MODELLING

Recently, strong and well justified criticism has been directed toward the use of aeronautical-type wind tunnels for investigation of pressures on models of structures. In some cases, the results of such tests can be highly misleading.

Seemingly a more promising development is the use of the boundary layer wind tunnel large enough to accommodate structural model testing. At present, only two or three such tunnels probably exist. That at the Boundary Layer Wind Tunnel Laboratory at The University of Western Ontario is of this type.

The application of this type of study is worthwhile in the investigation of large, important, structures exposed to the wind.

An outline of the possible phases of a wind tunnel study for the design of a tall building is given below in Table 2. The design procedure is illustrated diagrammatically in Figs. 10 and 11.

Perhaps the principal virtue of this approach is the understanding that evolves of the real way in which a structure is likely to behave in service; this understanding cannot really be duplicated by artificial formulation of wind loading parameters. While significant economy can be achieved by better tailoring the material in a structure to meet its actual behaviour, the greatest economy is achieved by recognition of problems at the design stage rather than after the structure is in service. The approach allows a number of problems which so far have been left unsettled to be studied; in particular, these problems include the question of maximum deflections, maximum acceleration, and the susceptibility of the structure to fatigue.

BIBLIOGRAPHY

A. G. Davenport "New approaches to the design of structures against wind action". Proceedings of Canadian Structural Engineering Conference, Toronto 1968. Published by Canadian Institute of Steel Construction.

A. G. Davenport "Gust loading factors". Jnl. of Str. Div., Proc. of Am. Soc. Civ. Eng., Vol. 93, pp 12-34, June 1967.

L. E. Robertson "On tall buildings" in "Tall Buildings". Ed. A. Coull, B. Stafford-Smith, Pergamon Press, 1967.

A. G. Davenport "The estimation of load repetitions on structures with application to wind induced fatigue and overload". Paper presented at the RILEM Symposium on the "Effects of Repeated Loading of Materials and Structures", Vol. 1, Mexico City, Sept. 15-17, 1966.

"Vejledning for fastsaettelse of vindbelastninger". Dansk ingeniorforenings standards for building construction, Teknisk Forlag, Kobenhavn, Denmark 1966.

M. Jensen, and N. Franck "Model scale tests in the natural wind, Part II", Danish Technical Press, Copenhagen, 1965.

International Conference on "Wind Effects on Buildings and Structures". NPL Teddington, England 1963, Pub. H.M.S.O., 1965.

International Seminar on "Wind Effects on Buildings and Structures". N.R.C., Ottawa, Canada, 1967, Proc. to be published by Univ. of Toronto Press.

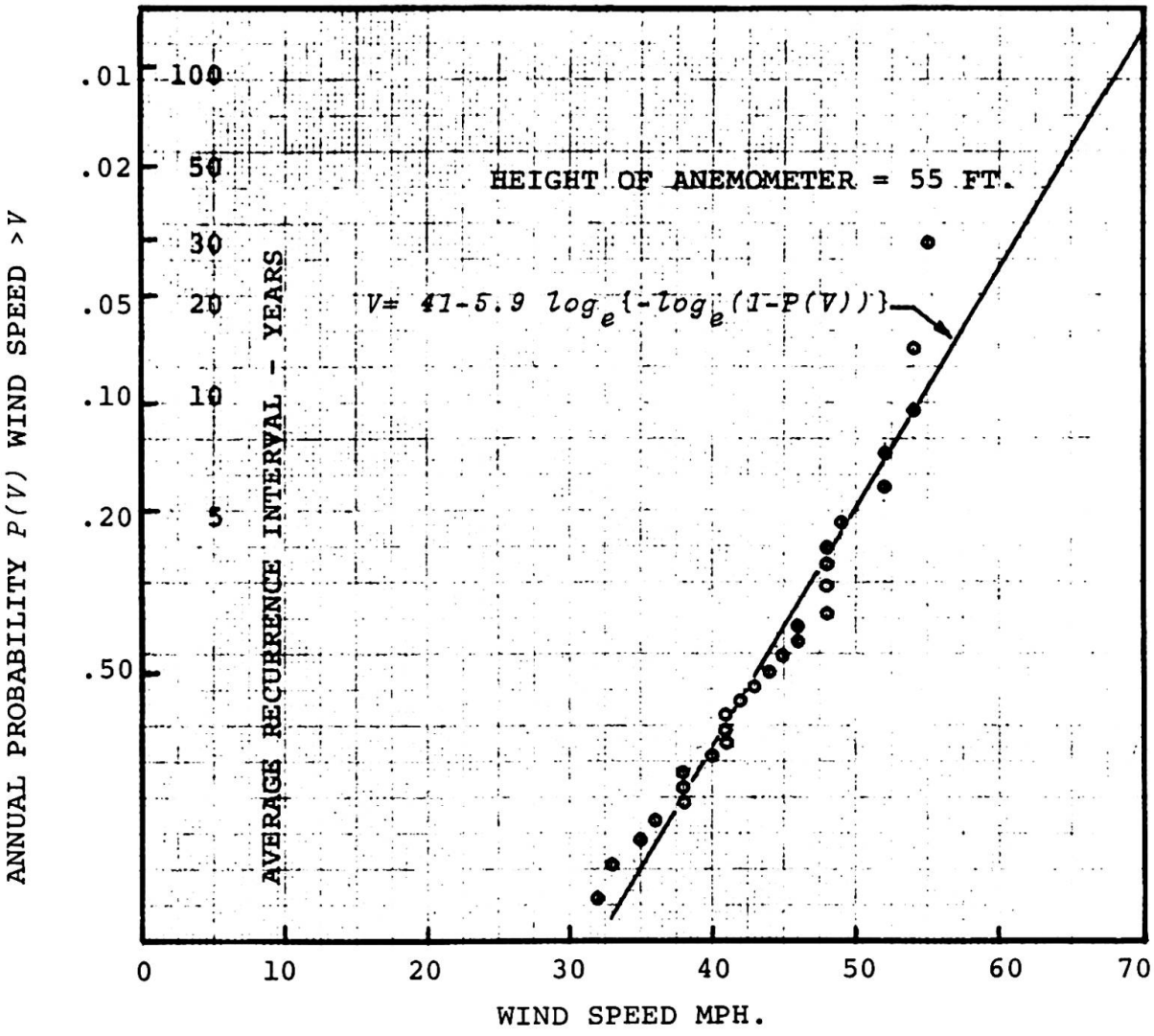

FIG. 1. EXTREME ANNUAL HOURLY AVERAGE WIND SPEEDS AT TORONTO MALTON AIRPORT (1939-1965).

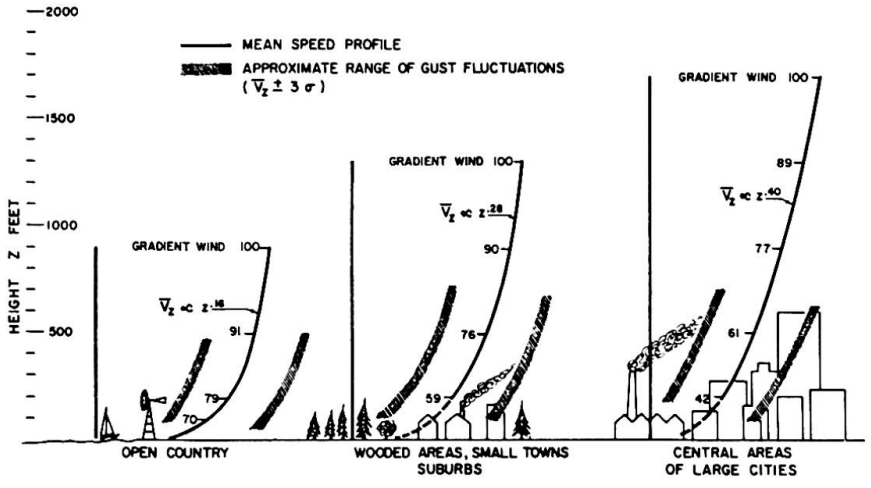

FIG. 2 MEAN WIND VELOCITY OVER LEVEL TERRAINS OF DIFFERING ROUGHNESS.

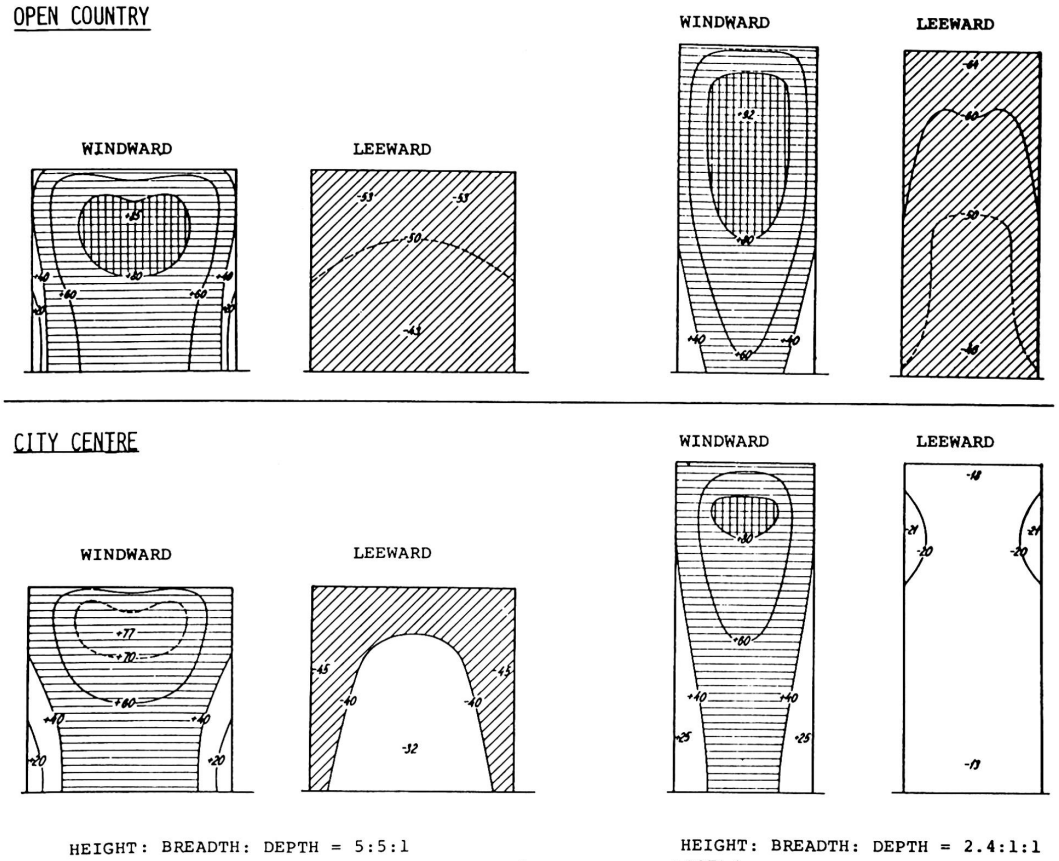

FIG. 3 TYPICAL AERODYNAMIC PRESSURE COEFFICIENTS (AFTER JENSEN-1965)(WIND NORMAL TO FACE: COEFFICIENTS REFERENCED TO VELOCITY PRESSURE AT ROOF LEVEL)

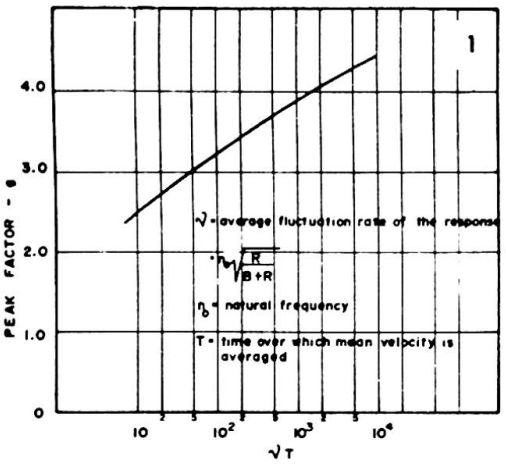

PEAK FACTOR

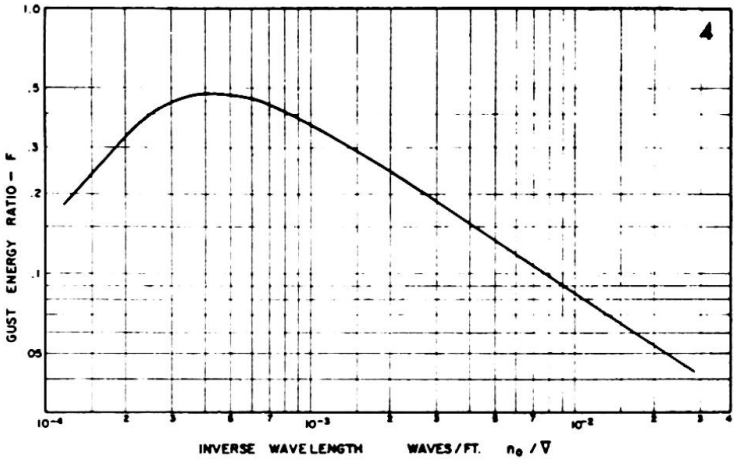

GUST ENERGY RATIO

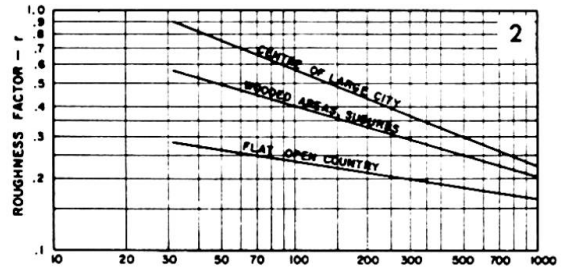

ROUGHNESS FACTOR

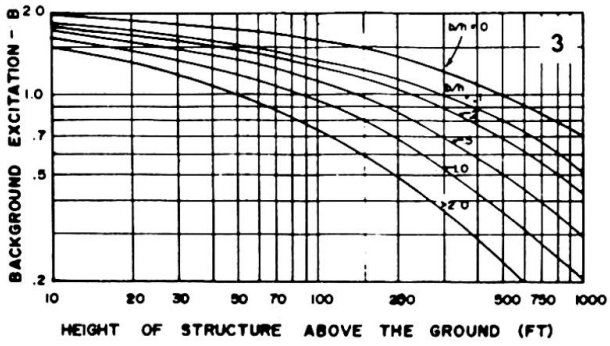

EXCITATION CAUSED BY BACKGROUND TURBULENCE

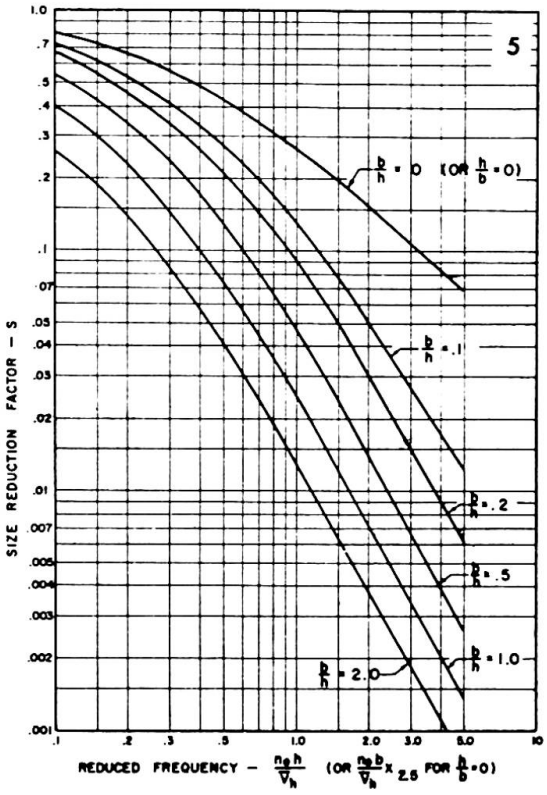

SIZE REDUCTION FACTOR

GUST FACTOR: $G = 1 + gr\sqrt{B+R}$ $\qquad R = \frac{SF}{\beta}$

FIG. 4

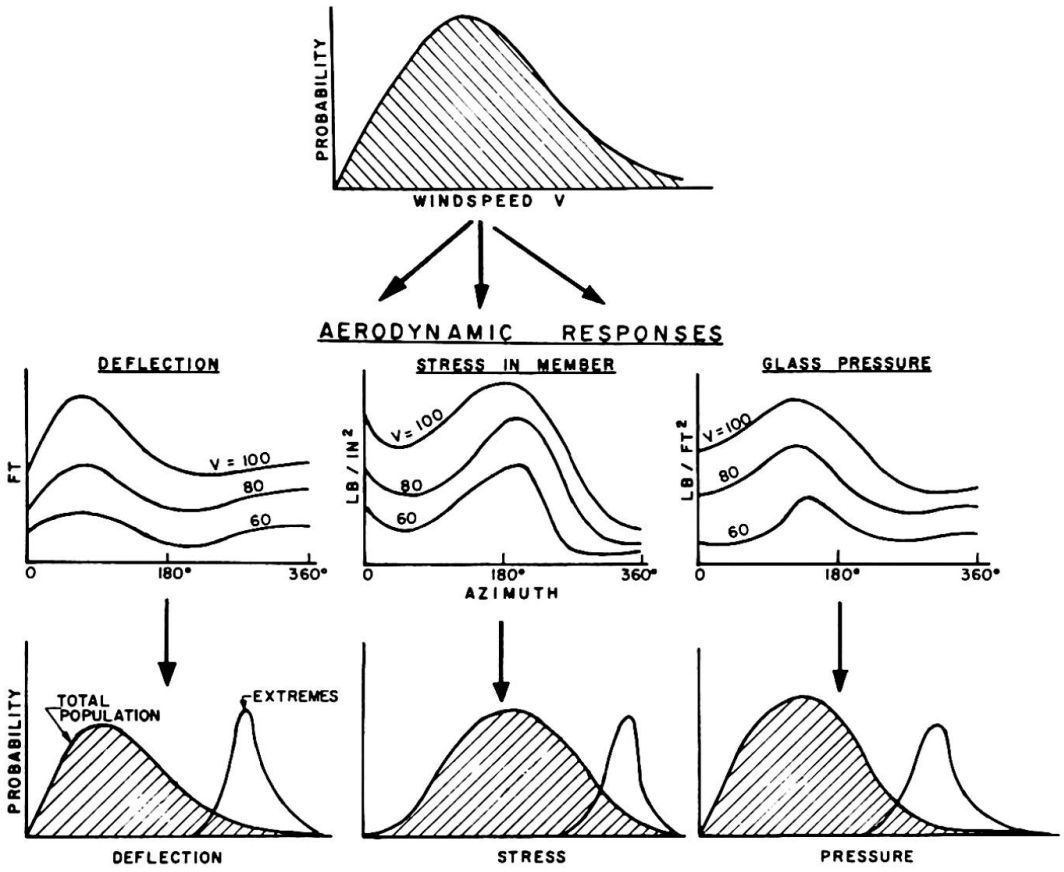

FIG. 5 DETERMINATION OF PROBABILITY DISTRIBUTIONS OF STRUCTURAL RESPONSE

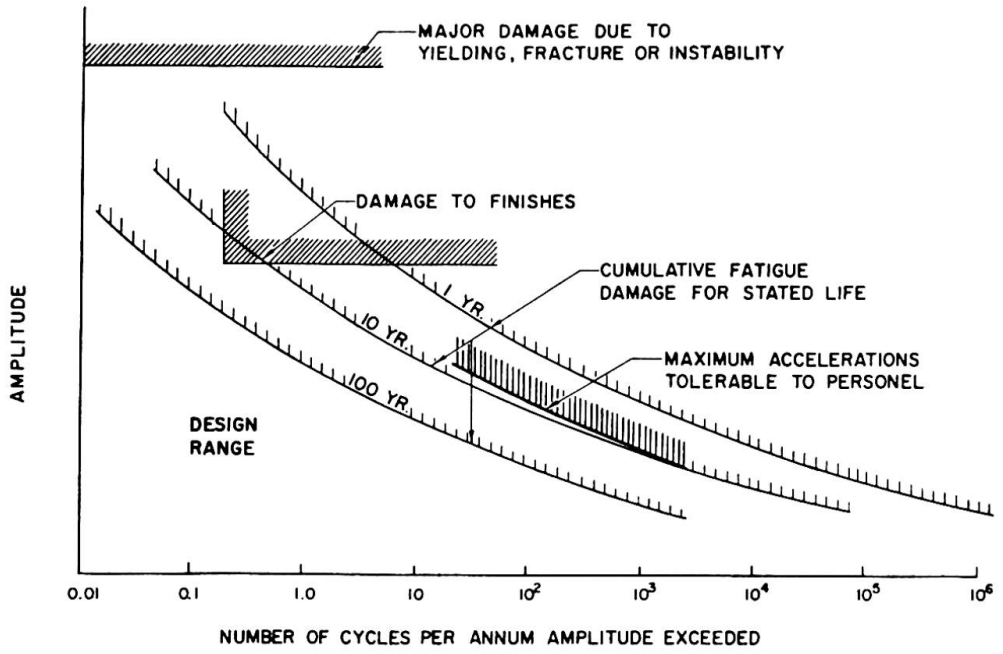

FIG. 6 ENVELOPE OF DESIGN LIMITATIONS